Designing genetically encoded probes to quantify nucleotide cofactors during the cell cycle in *Caulobacter crescentus*

A Thesis

submitted to

Indian Institute of Science Education and Research Pune in partial fulfilment of the requirements for the BS-MS Dual Degree Programme

by

Infas Raheem P
Roll. No: 20191182

Indian Institute of Science Education and Research Pune
Dr. Homi Bhabha Road,
Pashan, Pune 411008, INDIA.

Date: April, 2024

Under the guidance of

Dr. Sunish Radhakrishnan
Associate Professor
Department of Biology
IISER Pune

From May 2023 to Mar 2024

INDIAN INSTITUTE OF SCIENCE EDUCATION AND RESEARCH PUNE

Certificate

This is to certify that this dissertation entitled **“ Designing genetically encoded probes to quantify nucleotide cofactors during the cell cycle in *Caulobacter crescentus* ”** towards the partial fulfilment of the BS-MS dual degree programme at the Indian Institute of Science Education and Research, Pune represents study carried out by Infas Raheem P at Indian Institute of Science Education and Research, Pune under the supervision of Dr. Sunish Radhakrishnan, Associate Professor, Department of Biology, IISER Pune during the academic year 2023-2024.

Dr. Sunish Radhakrishnan

Committee:

Dr. Sunish Radhakrishnan

Dr. Amrita Hazra

Declaration

I hereby declare that the matter embodied in the report entitled **Designing genetically encoded probes to quantify nucleotide cofactors during the cell cycle in *Caulobacter crescentus*** are the results of the work carried out by me at the Department of Biology, Indian Institute of Science Education and Research, Pune, under the supervision of Dr. Sunish Radhakrishnan and the same has not been submitted elsewhere for any other degree. Wherever others contribute, every effort is made to indicate this clearly, with due reference to the literature and acknowledgement of collaborative research and discussions.

Infas Raheem P

20191182

Date: 27/03/2024

Table of Contents

List of Tables

List of Figures

Abstract

A recent study in *Caulobacter crescentus*, a dimorphic bacterial model to study cell cycle in prokaryotes, revealed the existence of a dynamic cytoplasmic redox and its importance in cell cycle progression. It was demonstrated that the cytoplasm of the swarmer (G1) cell remained reduced and a transition to oxidized state occurred during the G1 to S transition, which returned to reduced state at the G2/M phase. The importance of metabolic currencies such as NAD(P)(H) has been well documented to be involved in regulating the redox state of the cell. While NADH has been shown to cause an oxidative environment, NADPH has been demonstrated to act as a reducing equivalent for cells under oxidative stress. In *Caulobacter,* the status of NAD(P)(H) during the cell cycle, and redox oscillation, remains unexplored. Considering the influence of NAD(P)(H) on redox, it is likely that change in NAD(P)(H) levels could occur during the *Caulobacter* cell cycle. This study is focused towards designing genetically encoded sensors to measure the levels of nucleotide co-factors in live *Caulobacter* cells.

Acknowledgments

I am immensely thankful to Dr. Sunish Radhakrishnan for allowing me to join his lab for my Master's thesis. I am grateful to be part of his excellent research group and extremely interesting project. His constant guidance and mentoring enormously helped me to gain research insights and tremendously improved my skills and expertise.

I thank Shashank Agrawal for his patience, constant support, and motivation throughout this project. I thank him for motivating and enlightening me about how actual research should carry forward, how a researcher should move ahead, and how research should be conducted. He has precisely given the rightful guidance and support at the right moment. His work also showcased the importance of planning in research, which intrigued me more to be a researcher. He has given an immense boost to carry forward this project with many lessons and questions.

I want to thank Naveen Joseph Roy for gifting the chemicals needed for my project. I thank Aravind Gopi (SRF), for his valuable comments regarding my project and many actual realities inside a wet lab and how they help move researchers forward. He shared much of his experience, which motivated me to seek the answer in all directions possible and to learn what to look at before doing anything.

I want to thank graduate students in our lab, Hilal Ganie, Arnab Kumar Shau, Unnimaya AL, Richa Sarkar, Surbhi Yadav, and Manish Siwach, for helping me clear my doubts, demonstrations, and understanding new different techniques and their relevance in the field. In addition, I would like to thank my junior BS-MS students who rotated in our lab for having exciting discussions and debates regarding different relevant topics in biology. Also, they have helped me to revisit many fundamentals of biology and its current opinions.

I want to thank IISER Pune for providing good facilities, infrastructure, and support and allowing me to study. I also thank IISER Pune for the exposure given to me for pursuing science as a career in the future.

I want to thank all the past and present lab mates in the Sunish lab, Gayathri lab, and Sai Krishnan lab for helping me in different ways possible and providing an excellent environment for work. I want to thank the kho–kho team of 2023 -2024, who gave me a different vibe and colourful experiences throughout this year.

Finally, I sincerely thank my family and friends for always being there, supporting me, and motivating me whenever needed.

Thank you

Contributions

Contributor name	Contributor role
Shashank Agrawal, Sunish Radhakrishnan	Conceptualization Ideas
Shashank Agrawal, Infas Raheem, Sunish Radhakrishnan	Methodology
	Software
	Validation
Infas Raheem, Shashank Agrawal, Sunish Radhakrishnan	Formal analysis
Infas Raheem, Shashank Agrawal	Investigation
Sunish Radhakrishnan	Resources
	Data Curation
Infas Raheem	Writing - original draft preparation
Shashank Agrawal, Infas Raheen	Writing - review and editing
	Visualization
Shashank Agrawal, Sunish Radhakrishnan	Supervision
	Project administration
Sunish Radhakrishnan	Funding acquisition

Chapter 1 : **Introduction**

The growth and differentiation in both eukaryotes and prokaryotes are highly coordinated and regulated events (Curtis and Brun, 2010). Bacterial cells have a well programmed cell cycle which is governed at both transcriptional and translational levels. Understanding the cell cycle and its regulation might help to resolve various challenges such as designing strategies to attenuate pathogenesis, engineering industrially relevant strains etc. *Caulobacter crescentus,* a fresh water dwelling alphaproteobacteria is an established model organism to study cell cycle in bacteria. Using density gradient centrifugation, *C. crescentus* can be synchronized and the G1 cells (swarmer cells), which can be used to study an entire cell cycle. *C. crescentus* has a dimorphic life cycle, wherein flagellated swarmer cells search for nutrients. Upon encountering nutrient availability, the swarmer cells transition into an adherent stalked cell triggering replication and proliferation (**Fig. 1.1**). The replicating stalked cell eventually divides giving rise to a swarmer and a stalked daughter cell (**Fig. 1.1**) (Shapiro *et al.*, 1971; Curtis and Brun, 2010).

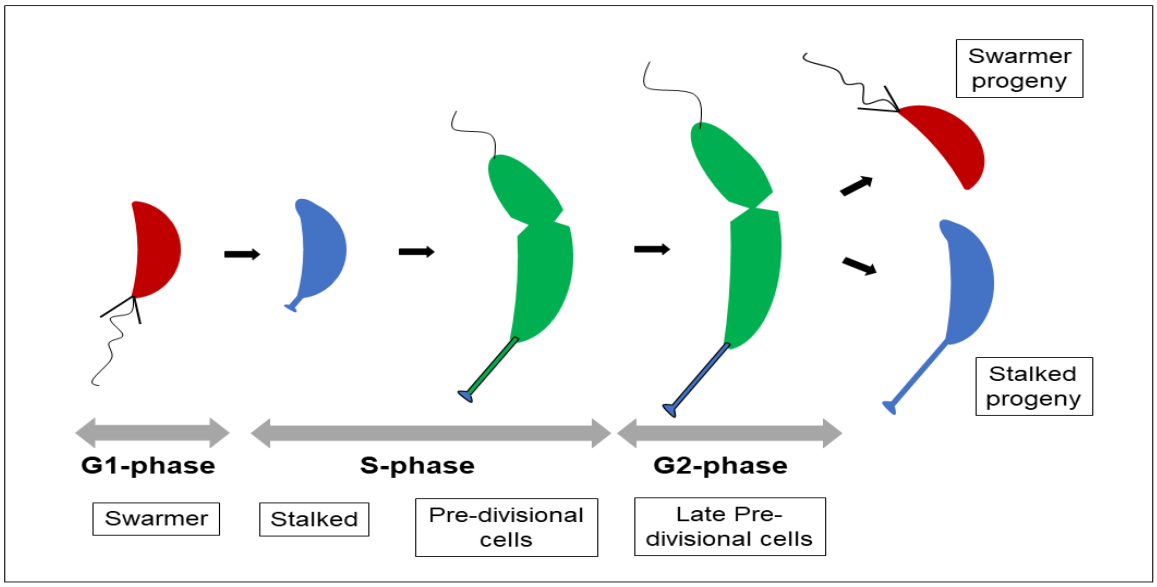

Figure 1. 1: Diagrammatic representation of cell cycle progression in *C. crescentus* : The red, blue and green coloured cells indicate swarmer cells, stalked cells and pre-divisional cells respectively. The cell cycle starts with G1 phase, where the swarmer cells eject flagella to generate stalks. The stalked cells (S-phase) grow and forms an asymmetric division and a flagellum at opposite end to give pre-divisional cells. Further, G2-phase is represented by late pre-divisional cells which eventually divide to produce swarmer and stalked progeny.

The precise control of cell cycle progression in *Caulobacter* is thorough the set of master transcriptional regulators, DnaA, CtrA and GcrA. These regulators are regulated both at the level of abundance and activity (Curtis and Brun, 2010).

Besides the above-mentioned regulators, a recent study from our group has shown the requirement of a dynamic cytoplasmic redox for proper cell cycle progression (Narayanan *et al.*, 2015). This study showed that the swarmer (G1) cells have a reduced cytoplasm and as cell enters into the S-phase, the cytoplasm becomes oxidised. Further, as the cell cycle proceeds, the restoration to reduced cytoplasm happens at the G2/M phase (**Fig. 1.2**). NstA, a repressor of the topoisomerase IV decatenation activity has been shown to be regulated at the level of activity thorough the formation of cysteine disulphides which is facilitated by the oxidised cytoplasmic environment (Narayanan *et al.*, 2015).

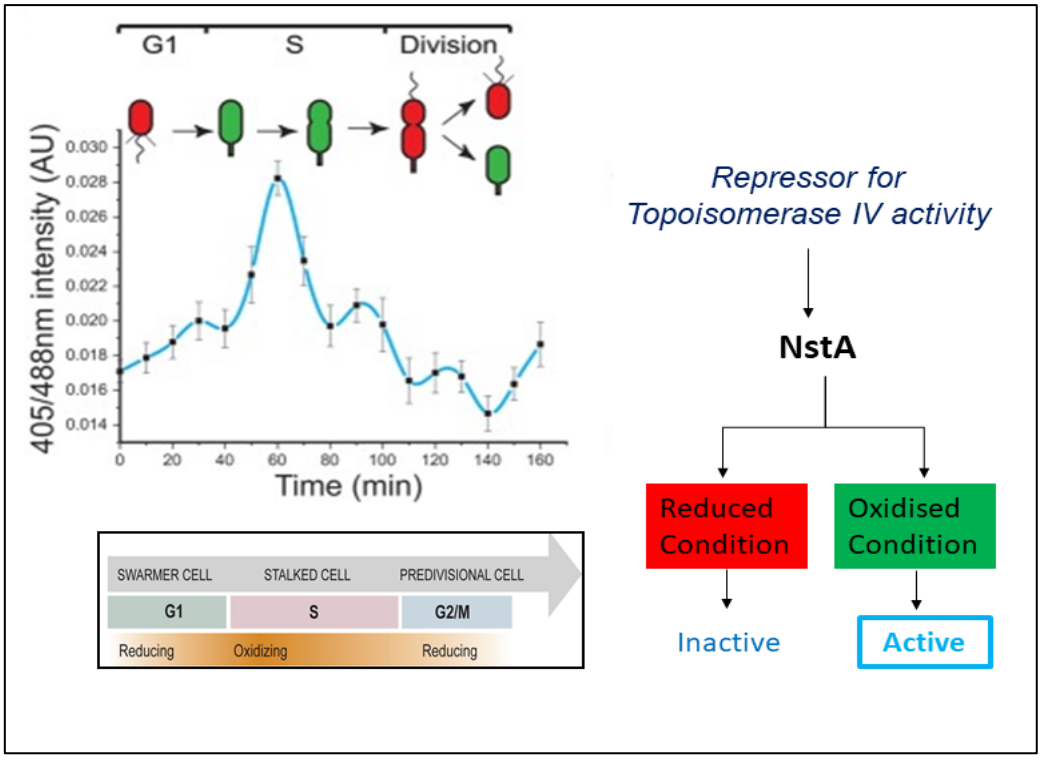

Figure 1. 2: Diagrammatic representation of intracellular redox oscillation through the cell cycle progression in *C. crescentus*: The cytoplasm of G1 cells is in reduced state. It becomes oxidised as the cell transitions into S-phase where NstA becomes active and then the cytoplasm become reduced when cell transitions into G2 phase where the NstA become inactive (adapted from *Narayanan et al, Genes&Dev, 2015*).

However, it is important for cells to manage the redox oscillations in the cytoplasm to prevent the detrimental effects of oxidative or reductive stress (Green and Paget,

2004). Importantly, how the redox oscillation is maintained during the cell cycle in *C. crecentus* is not explored. To gain a preliminary insight, we decided to monitor the factors that could induce the cytoplasmic redox change during the cell cycle. In general, reactive oxygen species (ROS) such as superoxide ion (O^{2-}), Hydrogen peroxide (H_2O_2), and hydroxyl radical ($HO^{\bullet}$), are well known factors, that causes oxidative stress (Messner and Imlay, 1999; Imlay, 2002). In addition to this, the nucleotide cofactor, NAD(H), has also been shown to induce oxidizing condition in cell. (Xie *et al.*, 2020). Conversely. the reduced condition in the cytoplasm is maintained by another nucleotide cofactor i.e. NADP(H), which serves as electron donor for Glutathione, a non-enzymatic antioxidant. (Sporer *et al.*, 2017). Therefore, it is imperative to measure the intracellular nucleotide cofactors NAD(H) and NADP(H), to gain insights into the redox changes.

At present, the most common methods/tools available for quantifying NAD(P)(H) employs spectrophotometric detection, enzymatic assays and HPLC (Lowry *et al.*, 1961; Umemura and Kimura, 2005; Vidugiriene *et al.*, 2014), which dependent on the efficiency of nucleotide extraction. Recently, genetically encoded sensors (GE sensors) conferring the advantage of *in vivo* measurements have evolved as a powerful tool to monitor changes in intracellular nucleotide levels in live cells (Wang *et al.*, 2023). GE sensors exhibit varied fluorescence behaviour upon nucleotide binding. These sensors majorly have two components (i) the circularly permuted fluorescent proteins (cpFPs) and (ii) a receptor having specificity to nucleotide-of-interest. Here, we have employed GE sensors, Peredox_mCherry (Hung *et al.*, 2011), PercevalHR (Tantama *et al.*, 2013) and Hyper7 (Pak *et al.*, 2020) for measuring intracellular NAD(H), ATP-ADP and H_2O_2, respectively.

These sensors are available commercially but need to be re-designed to make it compatible and functional in *C. crescentus*. In this study we are interested to design, construct, validate and measure the dynamicity of NAD(H), NADP(H), ATP and H_2O_2 during cell cycle in *C. crescentus* using the respective GE sensors.

Chapter 2 : **Materials and Methods**

2.1 Strains and growth conditions

The *C. crescentus* (NA1000) were cultured either in peptone yeast extract (PYE) rich medium [0.2% peptone, 0.1% yeast extract, 1mM $MgSO_4$ and 0.5 mM $CaCl_2$] or Glucose minimal medium, M2G (1X-M2 salt solution: 0.87 g/L Na_2HPO_4, 0.53 g/L KH_2PO_4, 0.25 g/L NH_4Cl), supplemented with 0.5 mM $MgSO_4$, 10 µM $FeSO_4$.EDTA, 0.5 mM $CaCl_2$ and 0.2% Glucose (Ely, 1991). The culture was incubated in rotatory shaker under 210 rpm in 29°C overnight till it reaches the required growth. Wherever required, kanamycin (5 µg/ml), vanillate induction of 0.5 mM (pH 7.5) was given for 4 hours and treated with FCCP (Carbonyl cyanide-p-trifluoromethoxyphenylhydrazone) (Sigma- #C2920), 25µM for 40 minutes.

The *Escherichia coli,* EC100 was used for cloning purpose and cultured in Luria Bertani (LB) medium (Hi-media). The culture was incubated in rotatory shaker under 210 rpm in 37°C overnight till it reaches the required OD. Wherever required, kanamycin (20 µg/ml) and agar (1.25%) were used.

2.2 Cell cycle synchronisation

The cells were grown in 10 mL M2G media overnight at 29 °C. The culture was diluted into fresh 200 ml M2G media and grown further till 0.4-0.6 OD is reached. The cells were pelleted at 5000 rpm for 5 minutes at 4 °C. The pellet was resuspended in 25 mL cold 1X-M2 salt and centrifuged at 8500 rpm for 2.5 minutes at 4 °C. The above step was repeated for two more times with 20 ml and 15 ml of cold 1X-M2 salt. The cells were finally resuspended in 5.6 ml of 1X-M2 salt and the 700 µL of cells were aliquoted into 8x 2 mL Microcentrifuge tubes. Next, 800 µL of Percoll (Cytiva) reagent was added to each 2mL vials with resuspended cells, mixed gently through the walls and centrifuged at 10000 rpm for 15 minutes at 4 °C. After centrifugation, two distinct layers of cells were formed, the upper layer corresponds to stalk and pre-divisional cells and the lower layer represented swarmer cells. The upper layer and supernatant were removed carefully and the lower layer was resuspended in 1mL of cold 1X-M2 salt. Cells were centrifuged at 8500 rpm for 2.5 minutes at 4 °C and removed the

supernatant. This step was repeated two more times and finally all the cells were concentrated into one 2 mL MCT and then pelleted by centrifugation at 8500 rpm for 4.5 minutes and the final pellet is resuspended in desired medium (Narayanan *et al.*, 2015).

Wherever required, the cells were grown in M2G till reading of 0.2 OD, then given induction of 0.5 mM vanillate (pH - 7.5) for 3-4 hours.

2.3 Plasmids and Primers used

The primers used in this study are tabulated below:

S.No.	Primer sequences	Primer name	Gene
1	5' AAAAAACATATGAAAGTTCCTGAAGCAGCCATT 3'	Peredox_mCherry Forward	Peredox_mCerry
2	5' AAAAAAGCTAGCTCACTTGTACAGTTCGTCCATGCC 3'	Peredox_mCherry Reverse	
3	5'AAAAAACATATGGAGGGCGGGCTGGGGCGTGCTG 3'	NADP-Snifit forward	NADP-Snifit
4	5' AAAAAAGCTAGCTTAAGCGGAAATTGAGGAGAAGCCCGGA 3'	NADP-Snifit reverse	
5	5' AAAGAACATATGAAAAAGGTGGAATCCATCATCAGG 3'	PercevalHR Forward	PercevalHR
6	5' AAAAAAGCTAGCTCACAGTGCTTCCTTGCCCTCCTCCTT 3'	PercevalHR reverse	
7	5' AAAAAACATATGGGATCCCGGGAATTCGCCACCATG 3'	Hyper7 Forward	Hyper7
8	5' AAAAAAGCTAGCTCAATCGCAGATGAAGCTAACACCA 3'	Hyper7 Reverse	
9	5′ GACGTCCGTTTGATTACGATCAAGATTGG 3′	pVan forward	NA
10	5′ GCCAGGGTTTTCCCAGTCACGA 3′	M13 Forward	NA

Table 2. 1 : List of primers designed for construction of GE sensors: The table shows the primers used for the GE sensor amplification having NdeI site at 5' position and NheI site at 3' position. The 9th and 10th primer were used to confirm the successful integration of the sensor inside the *C. crescentus* genome.

Plasmids used for this study are tabulated below:

S. No.	Name of plasmid	Source
1	pRsetB-His7tag-Peredox-mCherry	Addgene
2	pRsetB-PercevalHR	Addgene
3	pET-51b(+)_NADP-Snifit	Addgene
4	pQE30-HyPer7	Addgene
5	pV-Peredox-mCherryC-2	This study
6	pV-NADP-Snifit-C-2	This study
7	pV-PercevalHRC-2	This study
8	pV-Hyper7C-2	This study

Table 2. 2: List of plasmids used in this study: The plasmids- 1,2,3,4 was employed to amplify sensor proteins. Thus, used for the construction of desired GE sensors (5,6,7,8).

2.4 Polymerase chain reaction (PCR)

PCR (Bio-Rad T100^{TM} Thermal Cycler) is used for the amplification of the GE sensors and confirmation of successfully transformed strains.

After the amplification, the products are screened with 0.8% agarose gel electrophoresis added with EtBr (0.2-0.5 µg/mL.). Further downstream processes including gel purification, restriction digestion and ligation were done after the required band are amplified in the PCR.

2.5 Restriction digestion and ligation

The respective amplified GE sensor genes having NdeI site at 5' end and NheI site at 3' end was digested with respective restriction enzymes. these fragments were purified using the Qiagen gel clean-up kit and then ligated by two fragment ligations into pVVENC-2 which was digested with NdeI and NheI restriction enzymes. The ligated plasmid is transformed into a chemically competent EC100 cells using heat shock method and screened for positive colonies having kanamycin marker in LB-agar plate. The obtained colonies in the LB-kanamycin plate were screened using colony PCR, and confirmed colonies are grown in liquid LB media with kanamycin. From the culture,

the plasmid is isolated using a Qiagen mini-prep kit. The plasmid is sent for sequencing to check for point mutations.

2.6 Electroporation

The *C. crescentus* (NA1000) cells were electroporated with respective constructed plasmids having GE sensors with 1500V for 4 to 4.5 milli seconds and plated in PYE-agar plates supplied with kanamycin. The *C. crescentus* cells integrated with GE sensors were selected using kanamycin marker. Colonies were then grown in PYE broth with kanamycin.

2.7 Immunoblotting

The protein samples were resolved on 12.5 % sodium dodecyl sulphate polyacrylamide gel (SDS-PAGE) by applying constant voltage (100 V). Proteins were then transferred to a polyvinylidene difluoride membrane (PVDF, Millipore) at 4°C. The membrane was blocked with 5 % milk in the TBST buffer (20 mM Tris-HCl [pH 7.5], 150 mM NaCl, 0.1% Tween-20) for 1 hour at room temperature. Blots were then Incubated for 1-hour with monoclonal anti-GFP antibodies (Takara) (1:10,000 dilution) in TBST solution (20 mM Tris-HCl [pH 7.5], 150 mM NaCl, 0.1% Tween-20, 5% non-fat dry milk). Blots were then washed thrice with TBS buffer, followed by incubation with anti-mouse secondary antibody (Jackson ImmunoResearch) for one hour. Blots were washed thrice with TBS buffer again. Blots were developed using Clarity Western ECL substrate (Bio-Rad) and imaged on Cytiva Amersham Image quant 800 with an exposure time for 30 seconds.

2.8 Fluorescence acquisition using multimode reader

The measurement of the fluorescence was conducted using CLARIOstar plate reader (*BMG LabTech*).100 µL of the cells were added into 96 well black bottom plate (Nunc) with three technical replicates. For NADH/NAD^+ measurement (Peredox-mCherry) samples were excited with 400-15 nm and emission recorded at 510-20 nm with a dichroic filter of 490 nm. For the normalization of protein expression, mCherry was excited at 587-15 nm and emitted at 625-20nm with a dichroic filter 605 nm. The green

to red ratio from Peredox_mCherry is measured by taking the ratio of fluorescence from T-sapphire to mCherry after normalization to the blank.

Wherever required, the cells were pelleted with 9000 rpm for 3 minutes and resuspended in 1 mL of M2G van media before taking the measurement. Also, the culture as well as the blank was diluted to ten times in 1x M2 medium before taking 100 µL of culture for fluorescence acquisition.

For ATP/ADP measurement (PercevalHR-NA1000), the samples were excited with 490-15 nm and 420-15 nm with emission recorded at 530-20 nm and 525-15 nm respectively. The dichroic filter used are 508 nm and 495 nm for 490-15 nm and 420-15 nm excitation respectively. The ATP to ADP ratio is measured by taking the ratio of fluorescence from 490 nm excitation to 420 nm excitation after normalized to the blank. 200 µL of 0.8 OD G1 cells resuspended with M2G van media were added into the 96 well black bottom plate and allowed to grow in 29 °C with 500 rpm inside CLARIOstar plate reader and the measurement was taken at an interval of 10 minutes for 120 minutes using automation.

The graphs were plotted after taking the mean and standard error of the mean (SEM) of data from at least three independent experiments with blank normalization. The statistical analysis was done using unpaired parametric t-test.

Chapter 3 : **Results**

3. Construction of genetically encoded sensors for nucleotide cofactors and their measurement during the cell cycle in *C. crescentus*

Nucleotide cofactors such as NAD(H), NADP(H) could affect the cytoplasmic redox. It has been shown that NADP(H) is used by antioxidants such as glutathione and thioredoxin that maintain reduced condition of cytoplasm (Carmel-Harel and Storz, 2000). However, NAD(H) drives primarily oxidative reactions, thereby inducing oxidising condition (Xie *et al.*, 2020). In addition to that, since ATP/ADP ratio is the readout of the metabolism, therefore, we were also interested in quantifying ATP/ADP levels, thereby indicating the dynamicity of metabolism. Here, we employed fluorescent probes Peredox-mCherry, NADP-Snifit and PercevalHR to quantify NADH/NAD^+, NADPH/$NADP^+$ and ATP/ADP nucleotide cofactors respectively.

3.1 Construction of NAD(H) sensing probe in *C. crescentus* (Peredox-NA1000) and measuring NAD(H) during the cell cycle

Here, we employed Peredox_mCherry (pRsetB-His7tag-Peredox-mCherry) to quantify the NADH/NAD^+ ratio inside the cytoplasm (Hung *et al.*, 2011).In this study, we re-designed the Peredox-mCherry making it compatible for expression in *C. crescentus* and further quantified NAD(H) during cell cycle. Peredox_mCherry consists of two components, first, a NADH binding protein T-Rex having two dimers. Second, a pH resistant T-Sapphire protein (cpFP), which is linked between the T-Rex dimer. T-Sapphire gives the readout of cytoplasmic NADH/NAD^+ ratio due to the binding competition between NADH and NAD^+ with T-Rex protein. Binding of NAD^+ gives an open conformation whereas binding of NADH gives a closed confirmation leading to increased fluorescence from T-sapphire (green fluorescence) (**Fig. 3.1**) (Hung *et al.*, 2011). The probe is linked with mCherry (red fluorescence) as a control for the protein copy number since mCherry fluoresces irrespective of the NADH binding. NADH/NAD^+ ratio is quantified by calculating the green to red ratio.

We have chosen this sensor for the quantification because of the following advantage given by this probe. One, it is having pH resistant fluorescent protein T-sapphire and the second it is highly sensitive to NADH, as it can read even less than 5 nM NADH. Furthermore, green to red ratio can go up to ~2.5-fold increase suggesting its flexibility

in the scale. Therefore, it is a fast, efficient and robust tool to measure the NADH/NAD$^+$ levels in oligotrophic bacteria like *C. crescentus*.

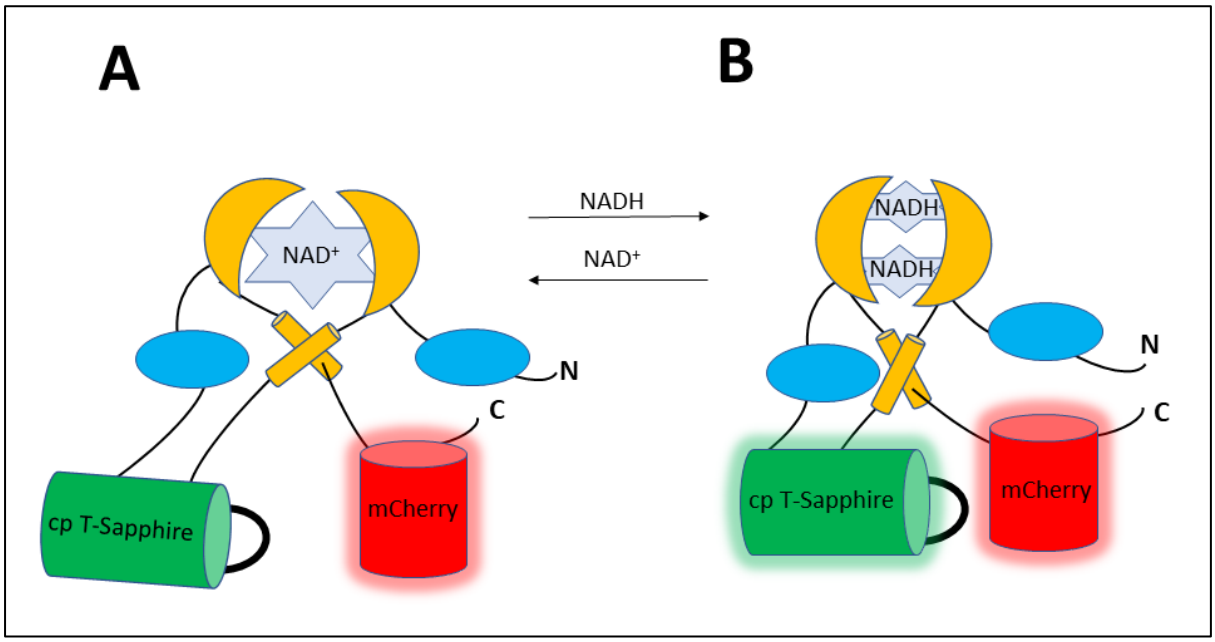

Figure 3. 1: Representation of NADH/NAD$^+$ sensing by Peredox_mCherry sensor. The diagram shows the existence of two confirmational states of Peredox_mCherry (having two homo dimer represented using blue and yellow) upon ligand binding where mCherry fluoresce irrespective of the ligand binding. **A)** Peredox_mCherry bound with NAD$^+$ ligand. **B)** Peredox_mCherry bound with NADH giving T-Sapphire to fluoresce. Figure made using information from Hung et al. 2011.

3.1.1 Designing pV-Peredox_mCherryC-2 construct sensing intracellular NAD(H)

pRsetB-His7tag-Peredox-mCherry plasmid detects NAD(H), which is compatible to *E. coli*. In order to have Peredox_mCherry suitable for expression inside the *C. crescentus.* we amplified the Peredox_mcherry gene from the above plasmid and inserted into pVVENC-2 plasmid (Thanbichler *et al.*, 2007). pVVENC-2 is high copy number plasmid with kanamycin resistant marker. Here, the gene of interest (Peredox_mCherry) is inserted downstream to vannillate promoter (Pvan) thereby, making the expression of Peredox_mCherry strictly under vanillate induction. Following above strategy, the sensor was constructed and named as pV-Peredox_mCherryC-2, the vector map of the same is shown in **Fig. 3.2**.

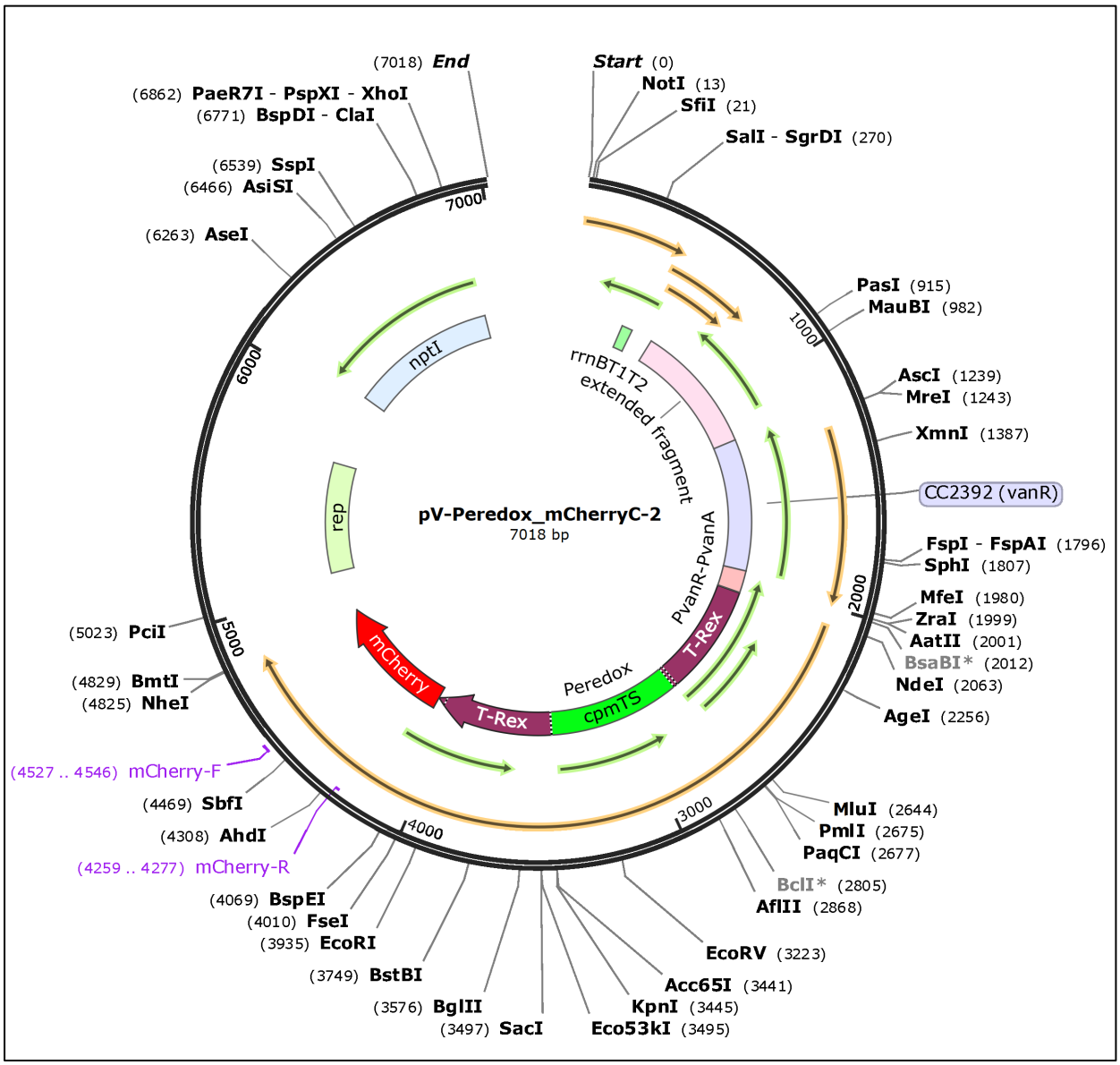

Figure 3. 2: Vector map of designed pV-Peredox_mCherryC-2 construct. The schematics shows the design of *C. crescentus* compatible integrative plasmid with Peredox_mCherry between NdeI and NheI downstream to vannilate promoter (7018 bp) (drawn using SnapGene).

3.1.2 Preparation of pV-Peredox_mCherryC-2 construct and its integration into the *C. crescentus* genome

The Peredox_mCherry gene i.e., T-Rex--T-sapphire--T-Rex--mCherry (2760 bp) is amplified from the template plasmid pRsetB-His7tag-Peredox-mCherry (**Fig. 3.3 a**). The obtained amplicon (2760 bp) was digested, and ligated into the vector pVVENC-2 and further transformed into EC100 (*E. coli*) cells (**Fig. 3.3 b**). The colonies obtained

after transformation were screened for cells harbouring pV-Peredox_mCherryC-2 construct (**Fig. 3.3 c**).

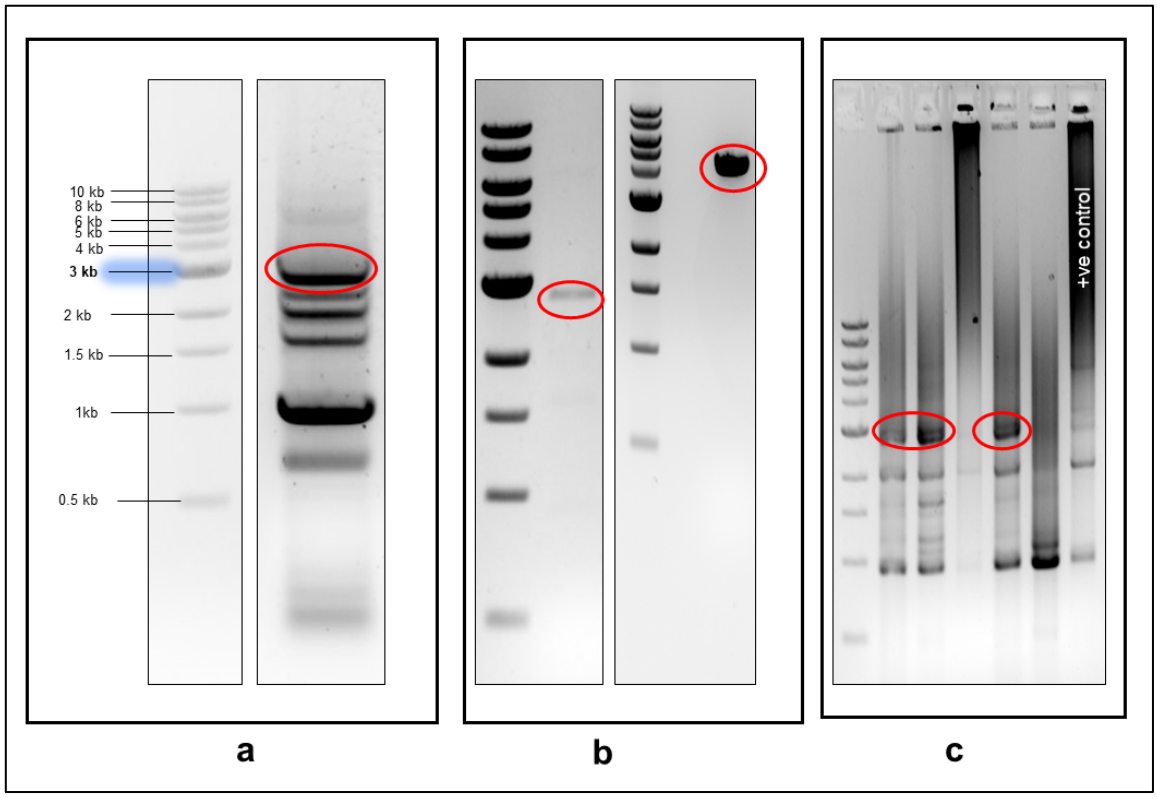

Figure 3. 3: Preparation of pV-Peredox_mCherryC-2 construct. The figure shows the agarose gel image for **a.** the PCR amplified product of the Peredox-mCherry gene (2.76 kb). **b.** Restriction digested product of Peredox-mCherry (left) and the plasmid pVVENC2 (4.258 kb) (right) with NdeI and NheI. **c.** the PCR screened EC100 colonies transformed with pV-Peredox_mCherryC-2. The requisite bands (2.76 kb) obtained were shown by red circle representing EC100 containing pV-Peredox_mCherryC-2 construct. Last lane is positive control that represents the amplification of Peredox_mCherry from the pRsetB-His7tag-Peredox-mCherry with the requisite band 2.76 kb.

The sequencing of the confirmed pVPeredox_mCherryC-2 plasmid was done and confirmed. The pV-Peredox_mCherryC-2 construct was then electroporated into NA1000 strain of *C. crescentus,* for its integration into the genome. To check, the integration of the Peredox_mCherry inside the vanillate locus of NA1000 we did colony PCR using out primers specific to the vanillate promoter (pvanF) upstream to the Peredox_mCherry gene and a M13F primer specific to the downstream of the gene (**Fig. 3.4).**

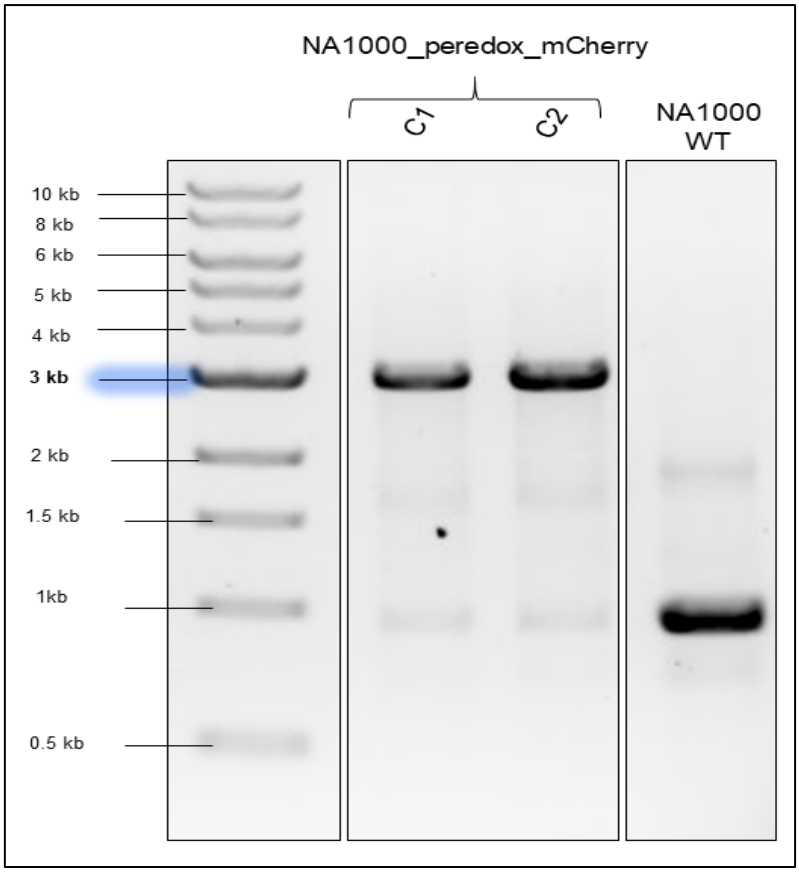

Figure 3. 4: Confirmatory PCR for screening the NA1000 cells integrated with Peredox-mCherry: The figure shows the agarose gel image for the PCR amplification of the Peredox-mCherry gene from the transformed NA1000 cells using the out primers pvanF and M13F. The requisite bands (2.89 kb) were obtained in colony 1 (C1) and colony 2 (C2) and NA1000 as negative control.

The *C. crescentus* cells harbouring Peredox-mCherry gene at Vanillate locus in the genome (here on, Peredox-NA1000) was confirmed and proceeded for the measurement of intracellular NAD(H).

3.1.3 Checking the expression of Peredox_mCherry gene in the engineered *C. crescentus* (Peredox-NA1000)

Before accessing the cytoplasmic NAD(H) levels, we first confirmed the expression of Peredox-mCherry from Peredox-NA1000 cells. Peredox-NA1000 cells were grown in minimal medium with Glucose (M2G) and induced with 0.5 mM vanillate (pH-7.5) for 4 hours. Further, the cells were collected and the expression of the Peredox_mCherry was checked by developing the immunoblot using monoclonal anti-GFP antibody. **Fig. 3.5** shows the immunoblot having the requisite band corresponding to

Peredox_mCherry (101kDa) protein under vanillate induction (+van). However, no band was obtained in an uninduced (-van) Peredox-NA1000 cells.

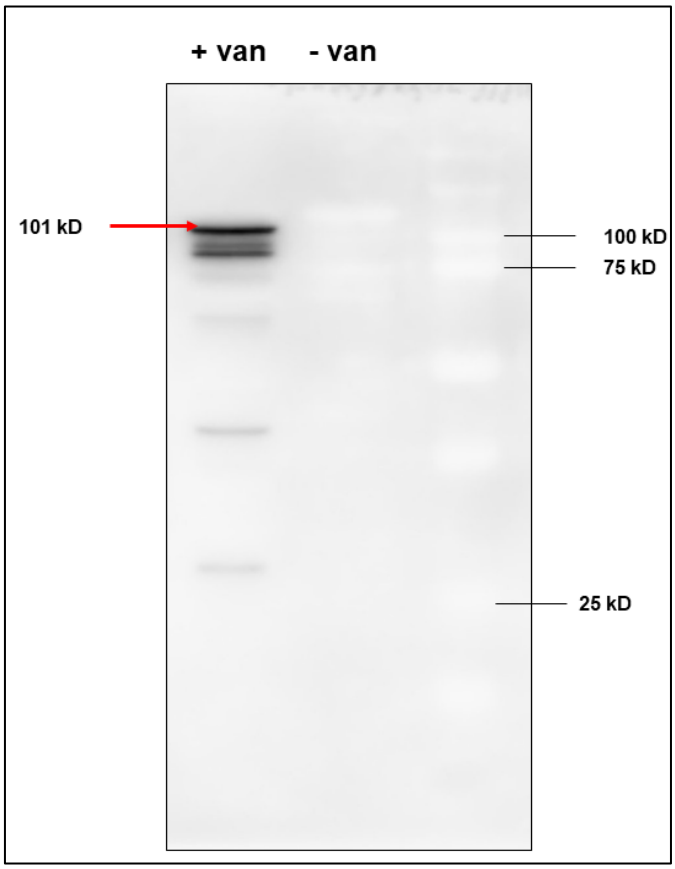

Figure 3. 5: Immunoblot showing the expression of Peredox_mCherry protein in Peredox-NA1000 cells. The figure shows the immunoblot for the Peredox-NA1000 cells expressing Peredox_mCherry protein (101 kDa) under 0.5mM vanillate (pH-7.5) induction for 4 hours. The blot was developed using monoclonal mouse antibody against GFP epitope.

3.1.4 Validation of Peredox_mCherry sensitivity to intracellular NAD(H) in the engineered *C. crescentus* (Peredox-NA1000)

Once we confirmed the expression of Peredox-mCherry protein, we next wanted to validate its sensitivity to detect NAD(H). For validation, here we have used FCCP (Carbonyl cyanide-p-trifluoromethoxyphenylhydrazone), an ionophore which is known to decreases the cytoplasmic NADH level in rat cardiomyocyte (Hu *et al.*, 2021). Peredox-NA1000 cells were induced for 3 hours with vanillate and treated with FCCP. Here we found that the treatment of 0.2 OD cells with the 25µM FCCP for 40 minutes showed a significant decrease in the intracellular NADH/NAD^+ ratio in *C. crescentus* (**Fig. 3.6**).

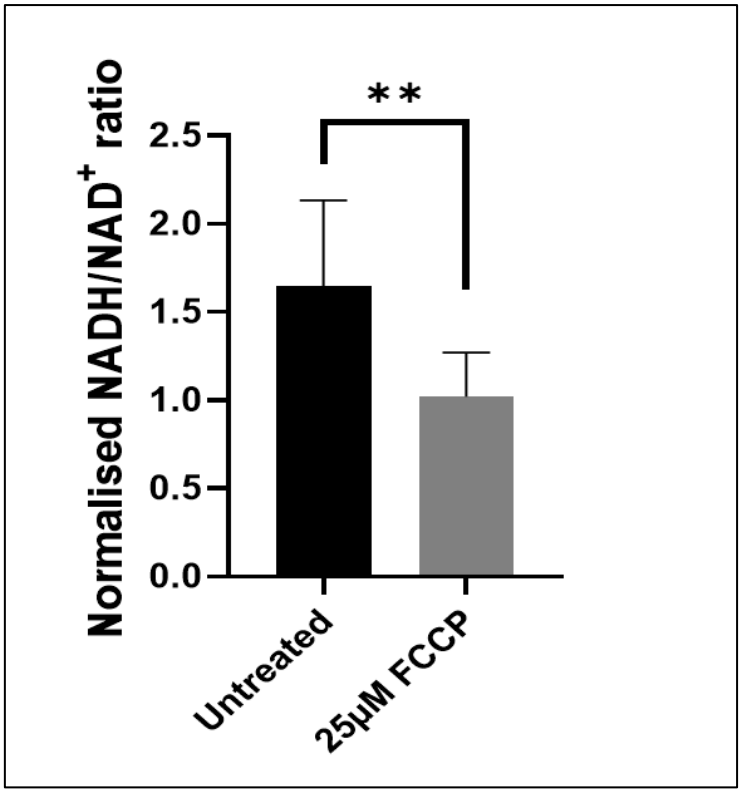

Figure 3. 6: Intracellular NADH/NAD$^+$ ratio in Peredox-NA1000 cells treated with FCCP. The figure shows significant decrease in NADH/NAD$^+$ ratio upon the treatment of 0.2 OD of cells with FCCP (25μM) for 40 min after Peredox_NA1000 cells were induced with 0.5 mM vanillate (pH-7.5) for 4 hours. Statistical analysis was done using unpaired parametric t-test conducted in four independent biological replicates where each contain two technical replicates (n=4, p-value=0.0085).

The treatment with FCCP showed that Peredox_NA1000 efficiently senses the NAD(H) levels and is suitable for measuring the intracellular NADH/NAD$^+$ ratio during the cell cycle in *C. crescentus*.

3.1.5 Measuring NADH/NAD$^+$ during the cell cycle in *C. crescentus*

The cytoplasmic redox oscillates during cell cycle in *C. crescentus* where among various factors, NAD(H), is a potent factor that could mediate redox changes. Here, we employed the Peredox-NA1000 cells to access the NAD(H) dynamics during cell cycle.

The Peredox-NA1000 cells were induced by Vanillate (van) for 3 hours and then was synchronized to separate the G1 cells. Next, the synchronized G1 cells (OD_{600} = 2) were allowed to grow in fresh M2G van medium and cell cycle was initiated. The cell cycle in M2G medium is prolonged for 120 minutes. To measure the intracellular

NAD(H) level, the cells were collected after diluted for 10 times in 1X M2 medium at the interval of 10 minutes and the fluorescence (Peredox-mCherry) was acquired as mentioned in the materials and methods. The fluorescence corresponding to NADH/NAD$^+$ ratio at each timepoint was then normalized to mCherry (representing the expression of Peredox-mCherry gene). The Normalized NADH/NAD$^+$ ratio obtained at each time point is plotted as shown in **Fig. 3.7**. Interestingly, our data showed that NADH/NAD$^+$ ratio changes during cell cycle. Where, the ratio is constant till mid S-phase and further it increases significantly after mid S-phase.

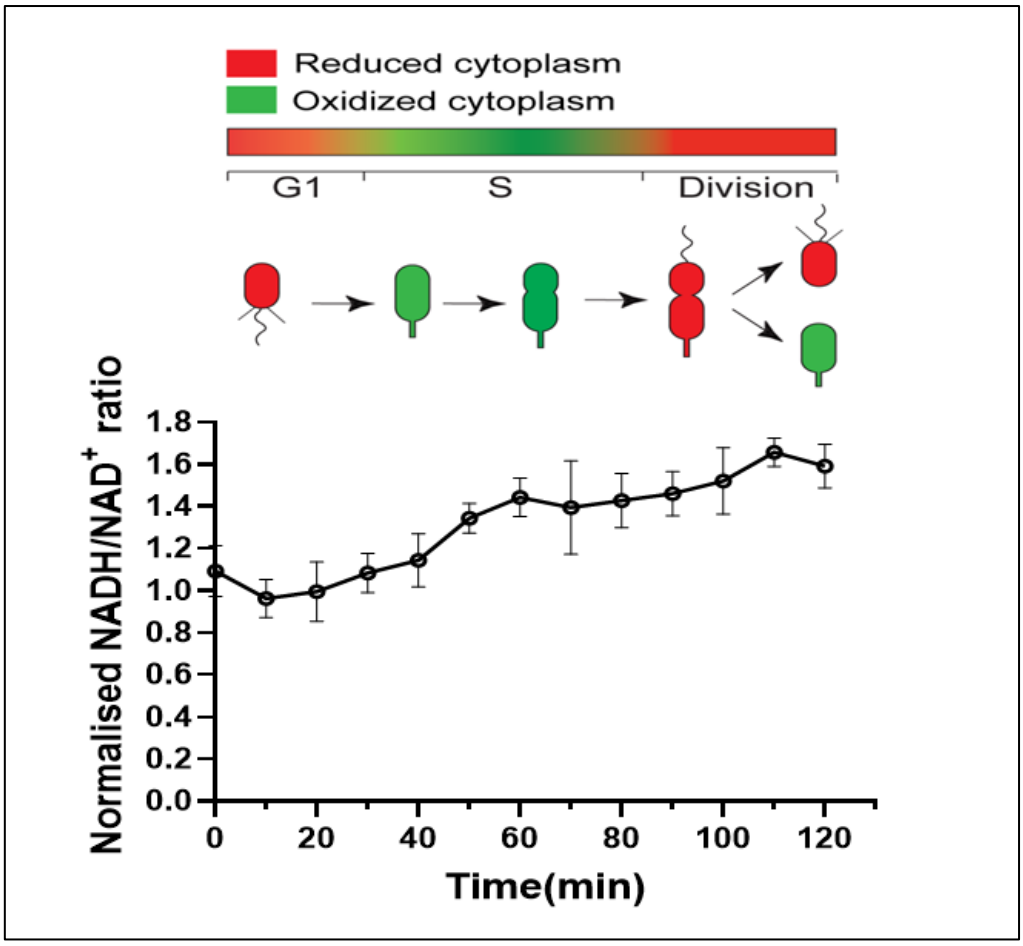

Figure 3. 7: Normalized NAD(H)/NAD$^+$ ratio levels during cell cycle in *C. crescentus*. The figure shows the NADH/NAD$^+$ ratio during the cell cycle progression in *C. crescentus*. 0.5 mM vanillate induction is given for 3 hours. The T-sapphire having an excitation of 400 nm and emission at 510 nm. mCherry fluorescence used for the normalising copy number have an excitation of 587 nm and an emission of 625 nm. The fluorescence was acquired at every 10 minutes and the graph was plotted using four independent biological experiments (n=4).

Importantly, our data revealed that the NADH/NAD$^+$ levels in cell is dynamic during the cell cycle and possibly effect the redox changes. Therefore, it provides an imperative

direction to investigate the contribution of NAD(H) in managing redox during cell cycle in *C. crescentus*.

3.2. Construction of NADP(H) sensing probe in *C. crescentus* (NADP-Snifit-NA1000) and measuring NADP(H) during the cell cycle

In order to measure the intracellular levels of NADPH/$NADP^+$ ratio, we have used the GE sensor, NADP-Snifit (Sallin *et al.*, 2018). It is a semisynthetic biosensor consists of NADP(H) binding protein i.e., Human Sepiapterin Reductase (SPR), synthetic labelling proteins Halo-tag and SNAP-tag attached using linkers. Additionally, two fluorophores are provided externally, first, SiR-Halo which binds to Halo-tag and the second is O^4-benzyl-2-chloro-6-aminopyrimidine tetramethyl rhodamine sulfamethoxazole (CP-TMR-SMX) that links with SNAP-tag. These two fluorophores act as FRET pair depending upon the binding of either NADP or NADPH with SPR. Whenever there is binding of NADPH, the sensor acquires an open structure enabling the fluorescence of TMR. Whereas when $NADP^+$ is bound to SPR the sensor acquires the closed confirmation thereby helping the TMR and SiR-Halo to come in FRET distance for resonance transfer of energy (**Fig. 3.8**) (Sallin *et al.*, 2018). The excitation for TMR is 520 nm and emission at 577nm, which will be increased when the sensor is bound to NADPH. However, in the presence of $NADP^+$ the SiR-Halo emits at 667 nm when excited with 520 nm. The emission of SiR-Halo at 667 nm is facilitated by closed confirmation of the sensor, which enable the FRET transfer from TMR to SiR-Halo. Therefore, considering the ratio of 577nm/667nm will indicate the NADPH/$NADP^+$ ratio in the cell (Sallin *et al.*, 2018).

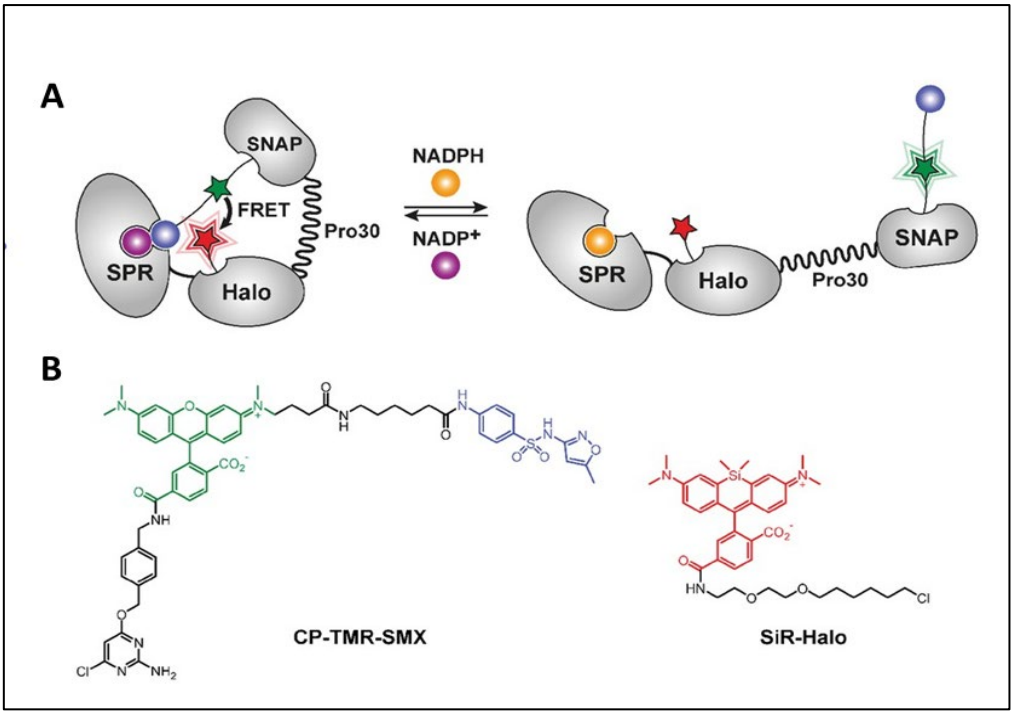

Figure 3. 8: Representation of NADPH/NADP$^+$ sensing by NADP-Snifit probe: (A) The figure shows the NADPH (yellow) bound state of NADP-Snifit (left) and NADP$^+$ (purple) bound state of NADP-Snifit (right) and the action of FRET by the help of the ligand sulfamethoxazole (blue). **(B)** Shows the chemical structure of the fluorescent dye where O^4-benzyl-2-chloro-6-aminopyrimidine tetramethyl rhodamine sulfamethoxazole (CP-TMR-SMX) is a derivative of tetramethyl rhodamine (green) dye linked with sulfamethoxazole (blue) as ligand and CP helps in labelling to SNAP-tag. SiR-Halo which is having silicon rhodamine (red) dye self-labels with Halo-Tag (Reproduced from *eLife, Sallin et al, 2018*).

This GE sensor is chosen for the quantification because of the following advantage given by this probe. One, it is a pH insensitive protein and have a large dynamic range of response towards the NADPH/NADP$^+$ ratio (half maximal response ratio = 30). Hence, it is an efficient and robust tool to measure the NADPH/NADP$^+$ levels in oligotrophic bacteria like *C. crescentus*.

3.2.1 Designing pV-NADP-SnifitC-2 construct for sensing intracellular NADP(H)

pET-51b(+)_NADP-Snifit plasmid detects NADP(H), which is compatible to *E. coli*. In order to have NADP-Snifit appropriate for expression inside the *C. crescentus.* we amplified the NADP-Snifit from the above plasmid and inserted into previously mentioned plasmid pVVENC-2. Here, the GE sensor NADP-Snifit is inserted downstream to Pvan thereby, making the expression of NADP-Snifit strictly under

vanillate induction. Following above strategy, the sensor was constructed and named the vector map as pV-NADP-SnifitC-2 shown in **Fig. 3.9**.

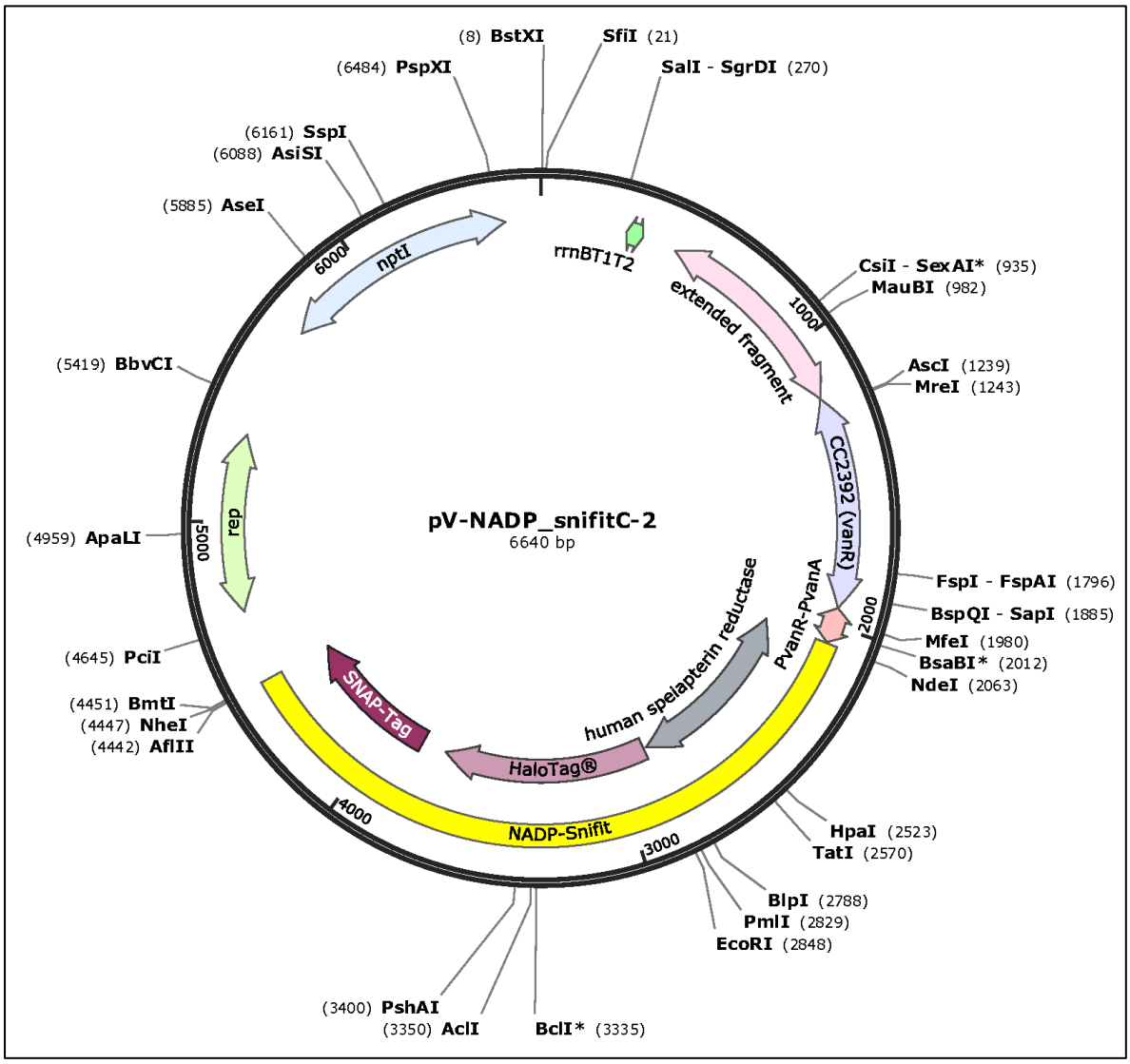

Figure 3. 9: Vector map of designed pV-NADP-SnifitC-2 construct. The schematics shows the design of *C. crescentus* compatible integrative plasmid with NADP-Snifit between NdeI and NheI downstream to vannilate promoter (6640 bp) (drawn using SnapGene).

3.2.2 Preparation of pV-NADP-SnifitC-2 construct and its integration into the *C. crescentus* genome

The NADP-Snifit gene consists of SPR linked with Halo-tag and SNAP Tag (2382 bp) is amplified from the template plasmid pET-51b (+) _NADP-Snifit (**Fig. 3.10 a**). The obtained amplicon (2382 bp) was digested, and ligated into the vector pVVENC2 and further transformed into EC100 (*E. coli*) cells (**Fig. 3.10 b**). The colonies obtained after

transformation were screened for cells harbouring pV-NADP-SnifitC-2 construct (**Fig. 3.10 c**).

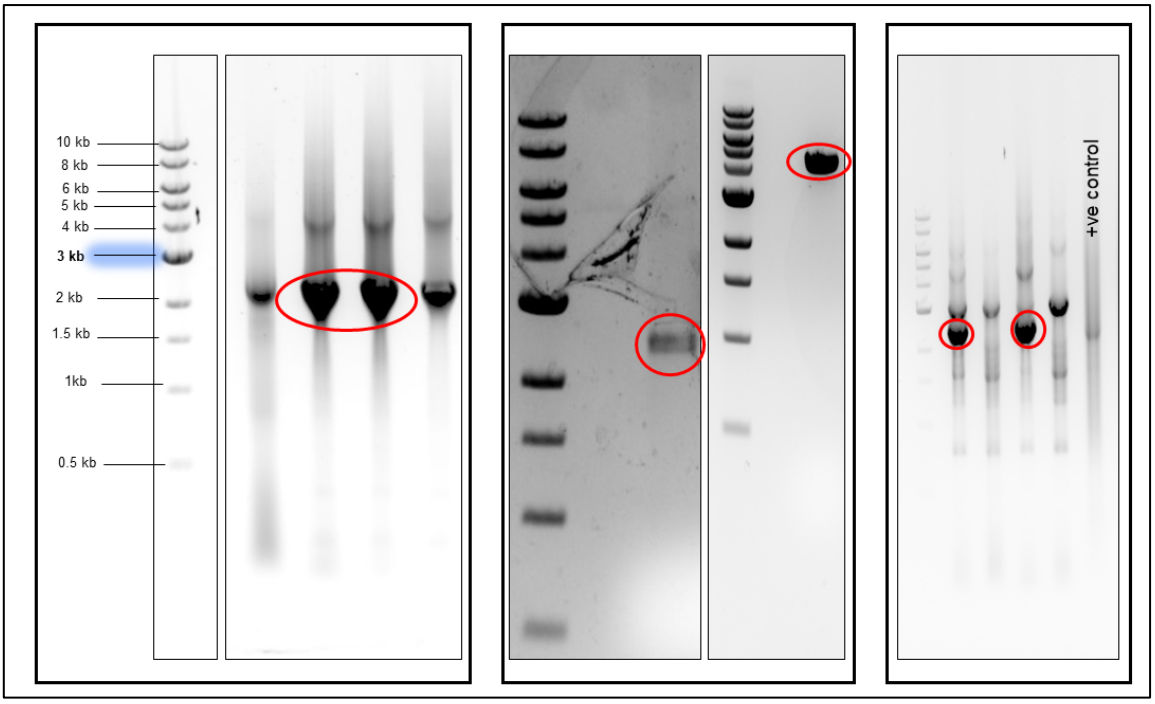

Figure 3. 10: Preparation of pV-NADP-SnifitC-2 construct. The figure shows the agarose gel image for **a.** the PCR amplified product of the NADP-Snifit gene from the template (2.382 kb). **b.** Restriction digested product of NADP-Snifit (left) and the plasmid pVVENC2 (4.258 kb) (right) with NdeI and NheI. **c.** the PCR-screened EC100 colonies transformed with pV-NADP-Snifit-C-2. The requisite bands (2.382 kb) obtained were shown by red circle representing EC100 containing pV-NADP-SnifitC-2 construct. Last lane is positive control that represents the amplification of NADP-Snifit from the pET-51b (+) _NADP-Snifit with the requisite band 2.382 kb.

Currently, we are in process of integrating the confirmed pV-NADP-SnifitC-2 into NA1000 genome. Once it is integrated further validation and measurement of NADPH/$NADP^+$ levels during the cell cycle would be conducted. The sequencing of the plasmid was done and confirmed.

3.3 Construction of ATP(ADP) sensing probe in *C. crescentus* (PercevalHR-NA1000) and measuring ATP/ADP ratio during the cell cycle

We have used the GE sensor PercevalHR to quantify the ATP/ADP ratio inside the cytoplasm (Tantama *et al.*, 2013). In this study we redesigned the PercevalHR making it compatible for expression in *C. crescentus* and further quantification during the cell cycle. PercevalHR consists of mVenus(cpFP) and ATP(ADP) binding protein GlnK.

GlnK1 has a T loop (Gly37- Val53) domain which will have conformational changes whenever there is a binding of Mg-ATP (Yildiz *et al.*, 2007). mVenus gives fluorescence at 420 nm when ADP is bound with the unordered structure of T loop. But whenever Mg-ATP is bound to the T-loop of GlnK forming an ordered structure helping mVenus giving increased excitation at 490 nm. The ATP/ADP ratio is due to the binding competition between the ATP and ADP in the T loop domain of GlnK **(Fig. 3.11)**. We have chosen this probe to quantify because this probe has a half maximal response value K_R ~3.5. i. e ATP/ADP ratio can go till 3.5-fold increase. Also, this probe is good in sensing the real time physiological values of ADP which was not the case about the earlier reported versions of Perceval.

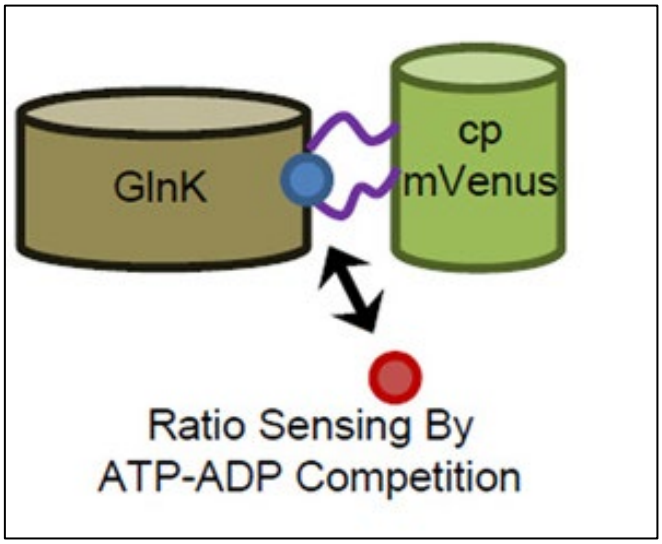

Figure 3. 11: Representation of ATP/ADP sensing by PercevalHR Sensor. The figure shows the sensor diagram where fluorescence is differed according to ATP-ADP sensing. Blue circle represents the ADP and the red circle represents the ATP. Upon ATP binding cpmVenus gives increased fluorescence at 490 nm (Reproduced from *Nature Comm, Tantama et al, 2013*).

3.3.1 Designing pV-PercevalHRC-2 construct sensing intracellular ATP(ADP)

pRsetB-PercevalHR plasmid detects ATP(ADP) which is compatible to *E. coli*. In order to have PercevalHR suitable for expression inside the *C. crescentus.* we amplified the PercevalHR gene from the above plasmid and inserted into pVVENC-2 plasmid. Here, the gene of interest (PercevalHR) is inserted downstream to Pvan thereby, making the expression of PercevalHR strictly under vanillate induction. Following above strategy, the sensor was constructed the vector map was named pVPercevalHRC-2 as shown in **Fig. 3.12**.

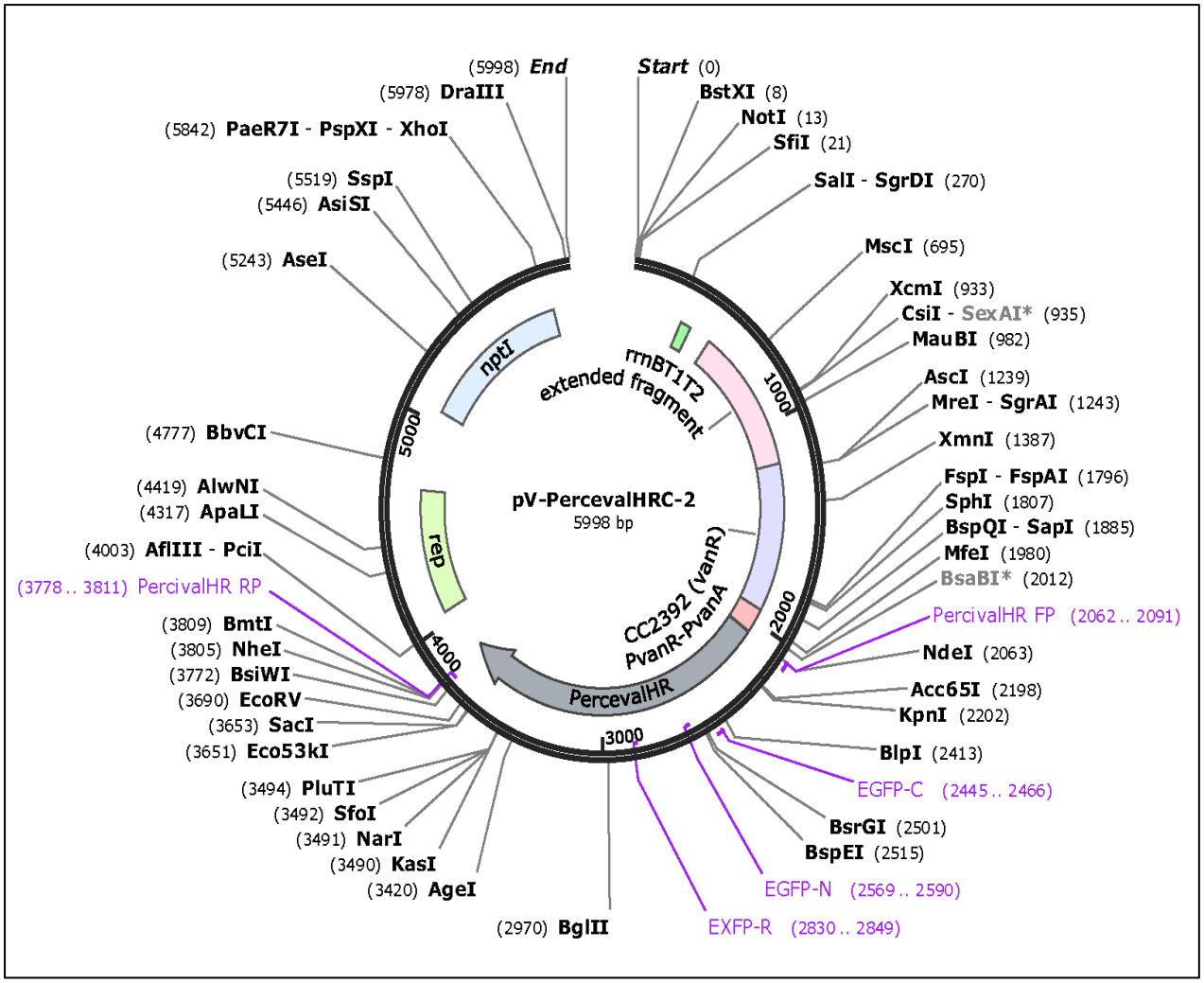

Figure 3. 12: Vector map of designed pV-PercevalHRC-2 construct. The schematics shows the design of *C. crescentus* compatible integrative plasmid with PercevalHR between NdeI and NheI downstream to vannilate promoter (5998 bp) (drawn using SnapGene).

3.3.2 Preparation of pV-PercevalHRC-2 construct and its integration into the *C. crescentus* genome

The PercevalHR gene consists of mVenus fused with GlnK1 in between T-loop (1740 bp) is amplified from the template plasmid pRsetB-PercevalHR (**Fig. 3.13 a**). The obtained amplicon (1740 bp) was digested, and ligated into the vector pVVENC-2 and further transformed into EC100 cells (**Fig. 3.13 b**). The colonies obtained after transformation were screened for cells harbouring pVPercevalHRC-2 construct (**Fig. 3.13 c**).

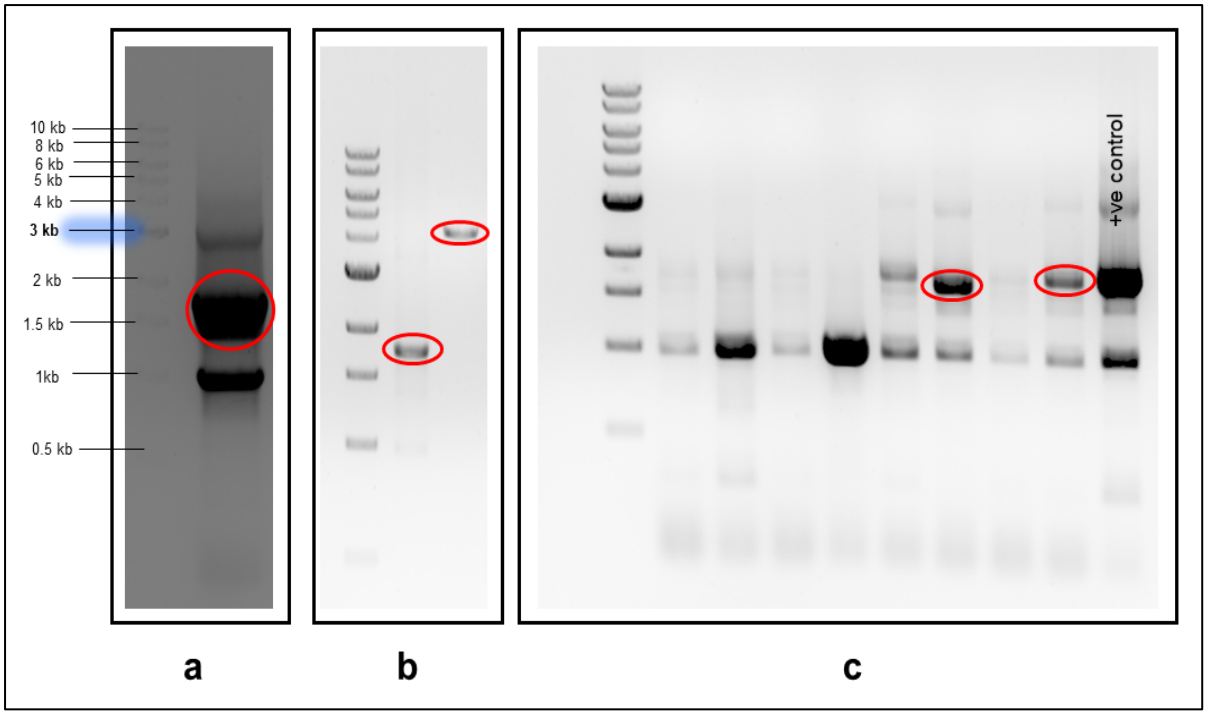

Figure 3. 13: Preparation of pV-PercevalHRC-2 construct. The figure shows the agarose gel image for **a.** the PCR amplified product of the PercevalHR gene (1.74 kb). **b**. Restriction digested product of PercevalHR (left) and the plasmid pVVENC2 (4.258 kb) (right). **c**. the PCR-screened EC100 colonies transformed with pV-PercevalHR. The requisite bands (1.740 kb) obtained were shown by red circle representing EC100 containing pV-PercevalHRC-2 construct. Last lane is positive control that represents the amplification of PercevalHR from the pRsetB-PercevalHR with the requisite band 1.74 kb.

The pVPercevalHRC-2 construct was then electroporated into NA1000 strain of *C. crescentus* for its integration into the genome. To check, the integration of the PercevalHR inside the vanillate locus of NA1000 we did colony PCR using out primers specific to the vanillate promoter (pvanF) upstream to the PercevalHR gene and a M13F primer specific to the downstream of the gene (**Fig. 3.14).**

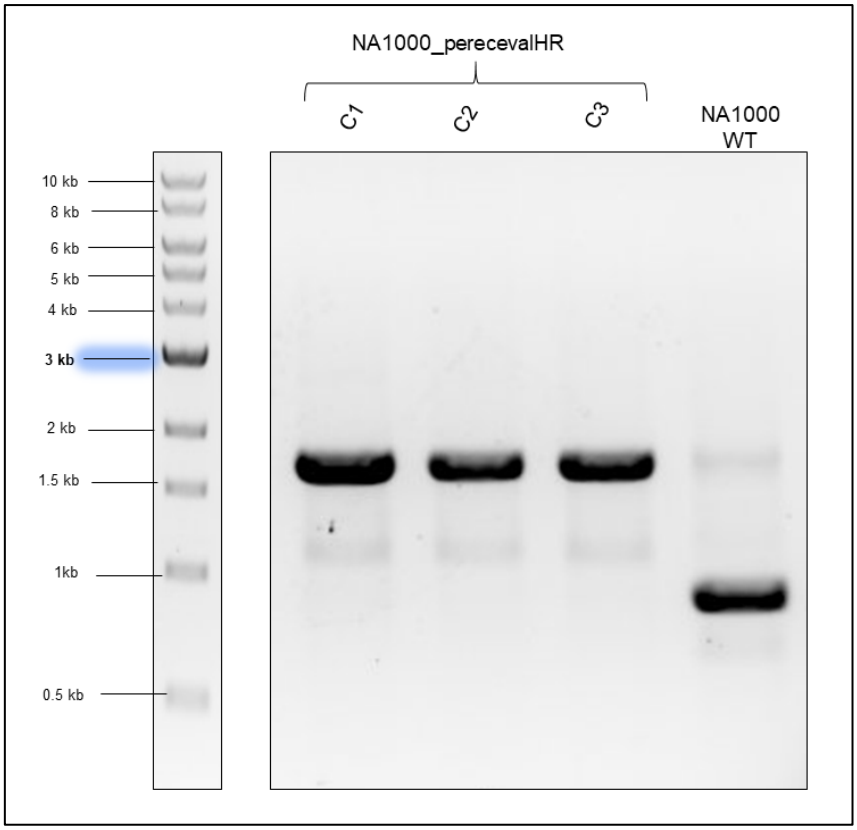

Figure 3. 14: Confirmatory PCR for screening the NA1000 cells integrated with PercevalHR. The figure shows the agarose gel image for the PCR amplification of the PercevalHR gene from the transformed NA1000 cells using the out primers pvanF and M13F. The requisite bands (1.87 kb) were obtained in colony 1 (C1) and colony 2 (C2) and NA1000 as negative control.

The *C. crescentus* cells harbouring PercevalHR at Vanillate locus in the genome (here on, PercevalHR-NA1000) was confirmed and proceeded for the measurement of intracellular ATP/ADP.

3.3.3 Checking the expression of PercevalHR gene in the engineered *C. crescentus* (PercevalHR-NA1000)

Before accessing the cytoplasmic ATP/ADP levels we first confirmed the expression of PercevalHR from PercevalHR-NA1000 cells. PercevalHR-NA1000 cells were grown in M2G and induced with 0.5 mM vanillate (pH-7.5) for 4 hours. Further, the cells were collected and to ensure the expression of the PercevalHR, we developed the immunoblot using monoclonal anti-GFP antibody. **Fig. 3.15** shows the immunoblot having the requisite band corresponding to PercevalHR (~ 62.5 kDa) protein under

vanillate induction (+van). However, no band was obtained in an uninduced (-van) PercevalHR-NA1000 cells.

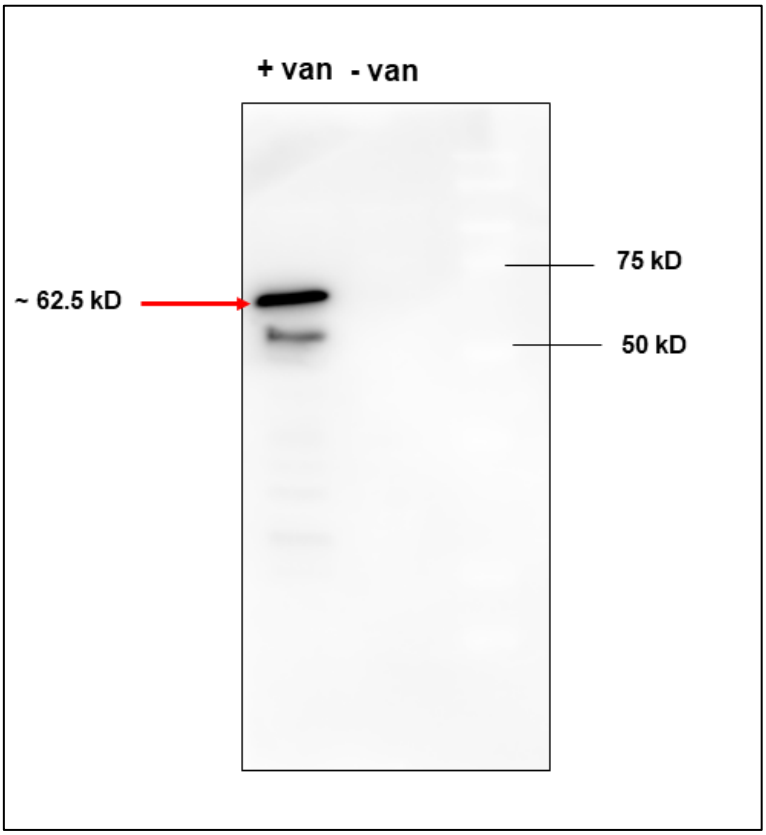

Figure 3. 15: Immunoblot showing the expression of PercevalHR protein in PercevalHR-NA1000 cells.The figure shows the immunoblot for the PercevalHR-NA1000 cells expressing PercevalHR protein (62.5 kDa) under 0.5mM vanillate (pH-7.5) induction for 4 hours. The blot was developed using monoclonal mouse antibody against GFP epitope.

3.3.4 Validation of PercevalHR sensitivity towards intracellular ATP(ADP) levels in the engineered *C. crescentus* (PercevalHR-NA1000)

Once we confirmed the expression of PercevalHR, we next wanted to validate its sensitivity to detect ATP(ADP). FCCP or CCCP (carbonyl cyanide *m*-chlorophenyl hydrazone) are the potent uncouplers for the ATP synthesis thereby disrupting electron motive force (Benz and McLaughlin, 1983). As a result, the ATP synthase cannot synthesize ATP and thus more ADP will be accumulated in the cell. It has been shown that in C. crescentus, the use of 25 µM of CCCP significantly perturbs the membrane potential without the cell lysis (Eun *et al.*, 2012). Hence, we treated 0.4 OD culture with the 25µM FCCP for 40 minutes. The cells were pelleted and resuspended in 1 mL M2G van and carried out for fluorescence measurement as discussed in

materials and methods. We found a significant decrease in ATP/ADP ratio in *C. crescentus* (**Fig 3.16**).

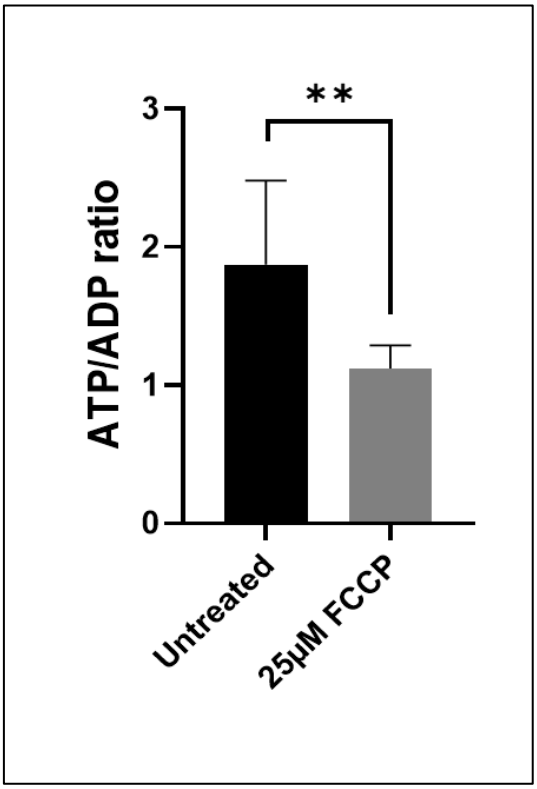

Figure 3. 16: Intracellular ATP/ADP ratio in PercevalHR-NA1000 cells treated with FCCP. The figure shows significant decrease in ATP/ADP ratio upon the treatment of FCCP (25μM) to 0.4 OD cells for 40 min after PercevalHR-NA1000 cells were induced with 0.5 mM vanillate (pH-7.5) for 4 hours. The statistical analysis was done using unpaired parametric t-test conducted in five independent biological replicates where each contain two technical replicates (n=5, p-value=0.0034).

The treatment with FCCP showed that PercevalHR-NA1000 efficiently senses the ATP(ADP) levels and is suitable for measuring the intracellular ATP/ADP ratio during the cell cycle in *C. crescentus*.

3.3.5 Measuring ATP/ADP during the cell cycle in *C. crescentus*

After validating the sensitivity of PercevalHR to ATP/ADP ratio inside the cytoplasm of *C. crescentus*. Next, we wanted to monitor the ATP/ADP ratio during the cell cycle.

For the estimation of ATP/ADP ratio, PercevalHR-NA1000 cells were synchronized and G1 cells with OD_{600} of 0.8 were resuspended in M2G van medium and cell cycle was initiated. Further, 200 μL cells were added into the 96 well black bottom plate in triplicates. The fluorescence was acquired for PercevalHR as mentioned in the method

section at an interval of 10 minutes. The fluorescence obtained was normalized with Blank (M2G van without cells) and ATP/ADP ratio was measured at each time point. The plot of individual fluorescence value corresponding ATP is shown in **Fig. 3.17.** We found that the ATP fluorescence increases from mid S-phase onwards whereas the ADP fluorescence increases linearly with the cell cycle progression.

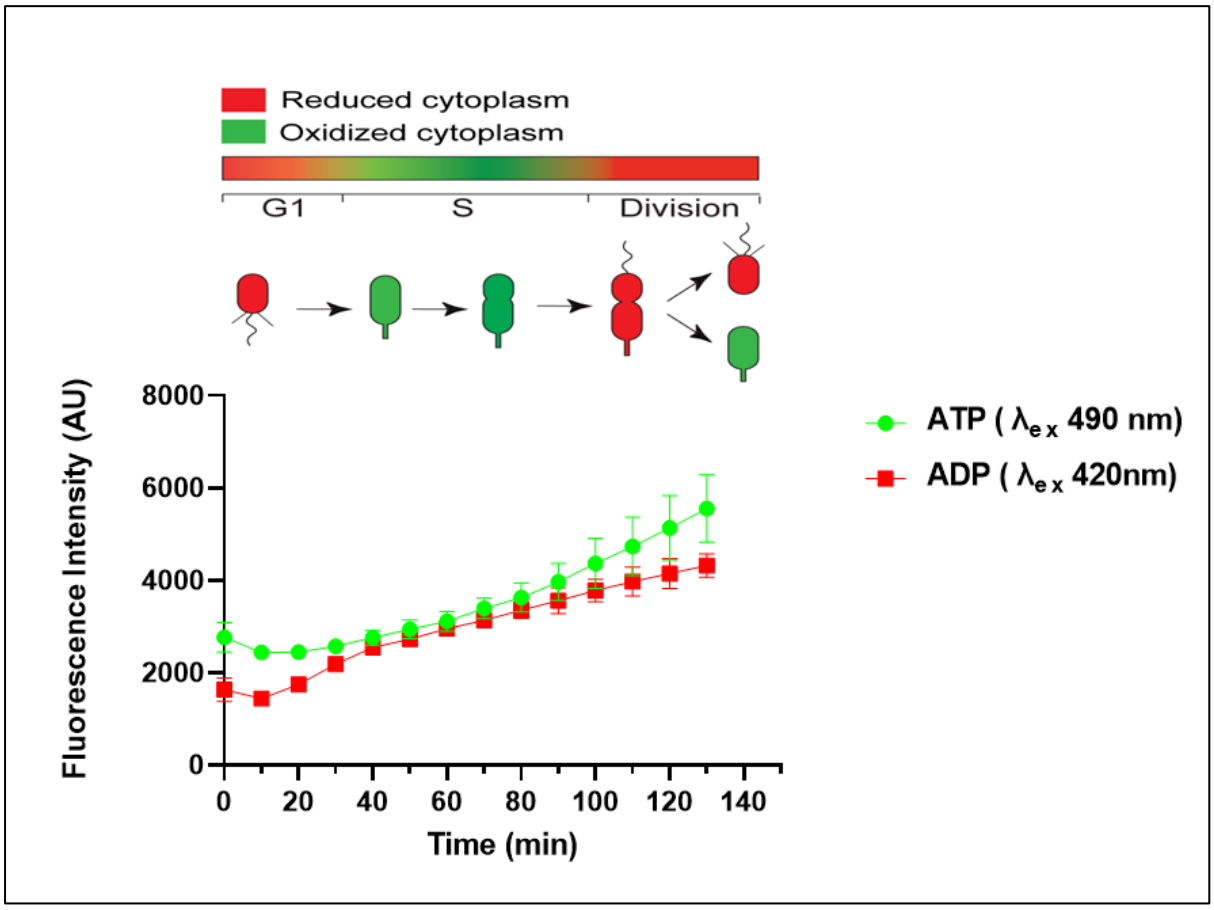

Figure 3. 17: ATP(ADP) fluorescence during cell cycle in *C. crescentus* using PercevalHR: The figure shows the fluorescence reading from λ_{ex}=490 nm (represents ATP) (green) and λ_{ex}=420 nm (represents ADP) (red) during the cell cycle of *C. crescentus* after 4 hours of 0.5 mM vanillate (pH-7.5) induction. Here, 0.8 OD of G1 cells were allowed to grow for the cell cycle progression in M2G van media. The fluorescence was acquired at every 10 minutes and the graph was plotted using three independent biological experiments (n=3).

The plot of ATP/ADP ratio is shown in **Fig. 3.18.** The ATP/ADP ratio decreases suddenly in initial phase of the cell cycle and become constant. Finally, an increase in the ATP/ADP ratio which start from late S-phase onwards.

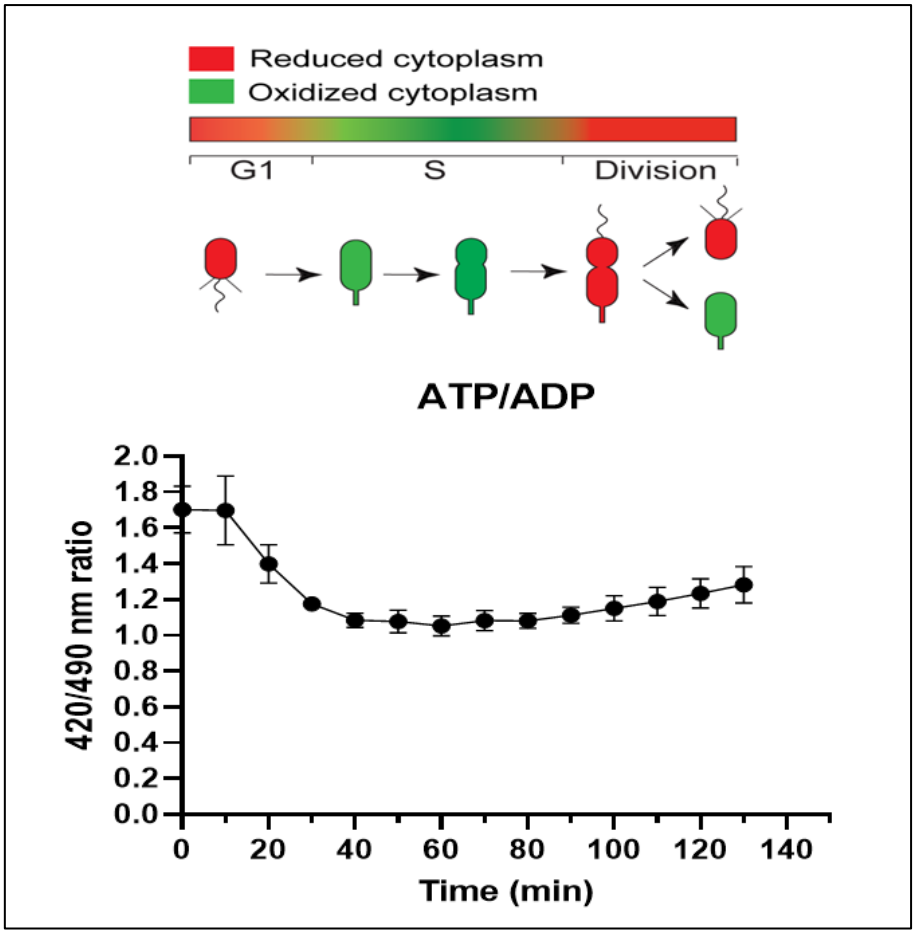

Figure 3. 18: ATP/ADP ratio during cell cycle using PercevalHR. The figure shows the ATP/ADP ratio during the cell cycle of *C. crescentus* after 4 hours of 0.5 mM vanillate (pH-7.5) induction. The ATP and ADP fluorescence acquired with 490nm and 420 nm excitation respectively with same emission of 530nm. Here, 0.8 OD of G1 cells were allowed to grow for the cell cycle progression in M2G van media. The fluorescence was acquired at every 10 minutes and the graph was plotted using three independent biological experiments (n=3).

Interestingly, we found that the ATP/ADP levels fluctuates during the cell cycle. This data suggest that ATP/ADP levels are dynamic during the cell cycle. In the initial part of the cell cycle there is a decrease in ATP/ADP levels suggesting a demand of ATP during the initial phase of the cell cycle. Further the ATP/ADP levels increases as the cell cycle proceeds. Although a greater number of replicates has to be conducted to establish this existing fluctuation of ATP/ADP during the cell cycle in *C. crescentus.*

3.4. Construction of H_2O_2 sensing probe in *C. crescentus* (Hyper7-NA1000) and measuring H_2O_2 during the cell cycle

Studies have shown that ROS species such as H_2O_2 induces the oxidative stress to the cell. The fluctuations in the H_2O_2 levels during the cell cycle in C. crescentus will be

fascinating to look into (Imlay, 2002; Ray *et al.*, 2012). Therefore, we use fluorescent probe Hyper7 to quantify the H_2O_2 levels during the cell cycle.

Here, we employed an ultrasensitive GE sensor, i.e., Hyper7 (pQE30-HyPer7), to quantify the H_2O_2 ratio inside the cytoplasm. In this study, we re-designed the Hyper7, making it compatible with expression in *C. crescentus* and further quantifying H_2O_2. Hyper7 is made of two components; first, a regulatory domain of H_2O_2 sensing protein OxyR (Oxy-RD). Second, a cpYFP protein (cpFP) is linked between 126-127 positions of Oxy-RD from *Neisseria meningitidis*. Hyper7 gives the readout based on H_2O_2 concentration, which in turn makes disulphide bond formation in Oxy-RD, enhancing the fluorescence from cpYFP (**Fig 3.19**) (Pak *et al.*, 2020). We have chosen this sensor for the quantification because of the following advantages given by this probe. One, it is a pH-resistant variant, and the second, its sensitivity to H_2O_2 concentration is in the range of 10nM. Hence, it is a fast, efficient and robust tool to measure the H_2O_2 levels in oligotrophic bacteria like *C. crescentus*.

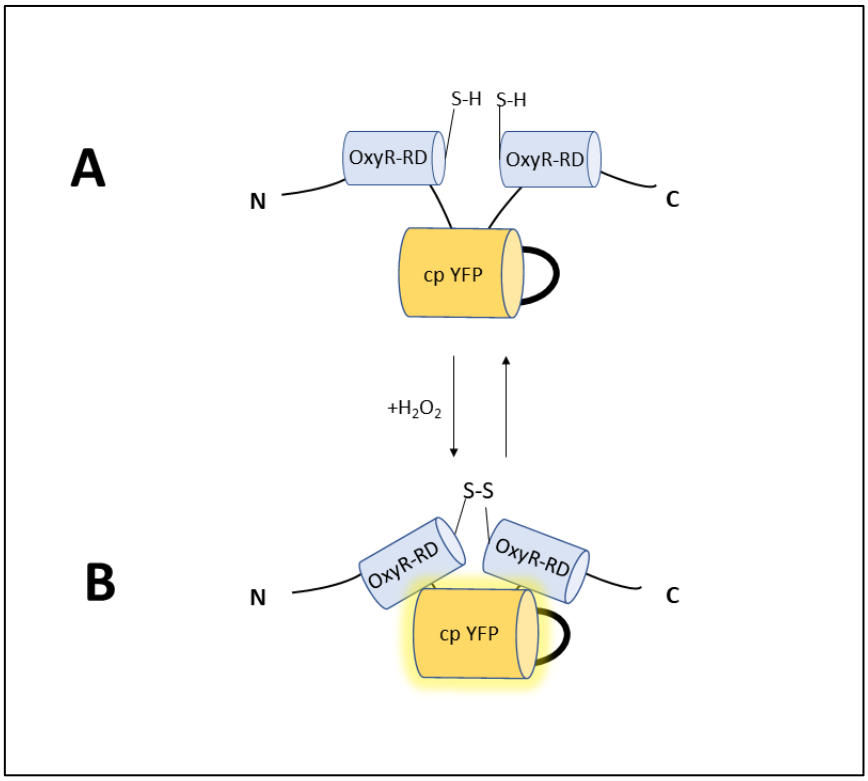

Figure 3. 19: Representation of H_2O_2 sensing by Hyper7 sensor. The diagram shows the existence of two confirmational states of Hyper7 upon ligand binding. **A)** Hyper7 sensor in absence of H_2O_2. **B)** Hyper7 sensor in presence of H_2O_2 catalysing disulphide bond giving rise to cpYFP to fluoresce. Drawn using information from Pak et al. 2020.

3.4.1 Designing pV-Hyper7C-2 construct sensing intracellular H_2O_2

pQE30-HyPer7 plasmid detects H_2O_2 which is compatible to *E. coli*. In order to have Hyper7 suitable for expression inside the *C. crecentus.* we amplified the Hyper7 from the above plasmid and inserted into pVVENC-2 plasmid. Here, the gene of interest (Hyper7) is inserted downstream to Pvan thereby, making the expression of Hyper7 strictly under vanillate induction. Following above strategy, the sensor was constructed and the vector map is named pV-Hyper7C-2 as shown in **Fig. 3.20**.

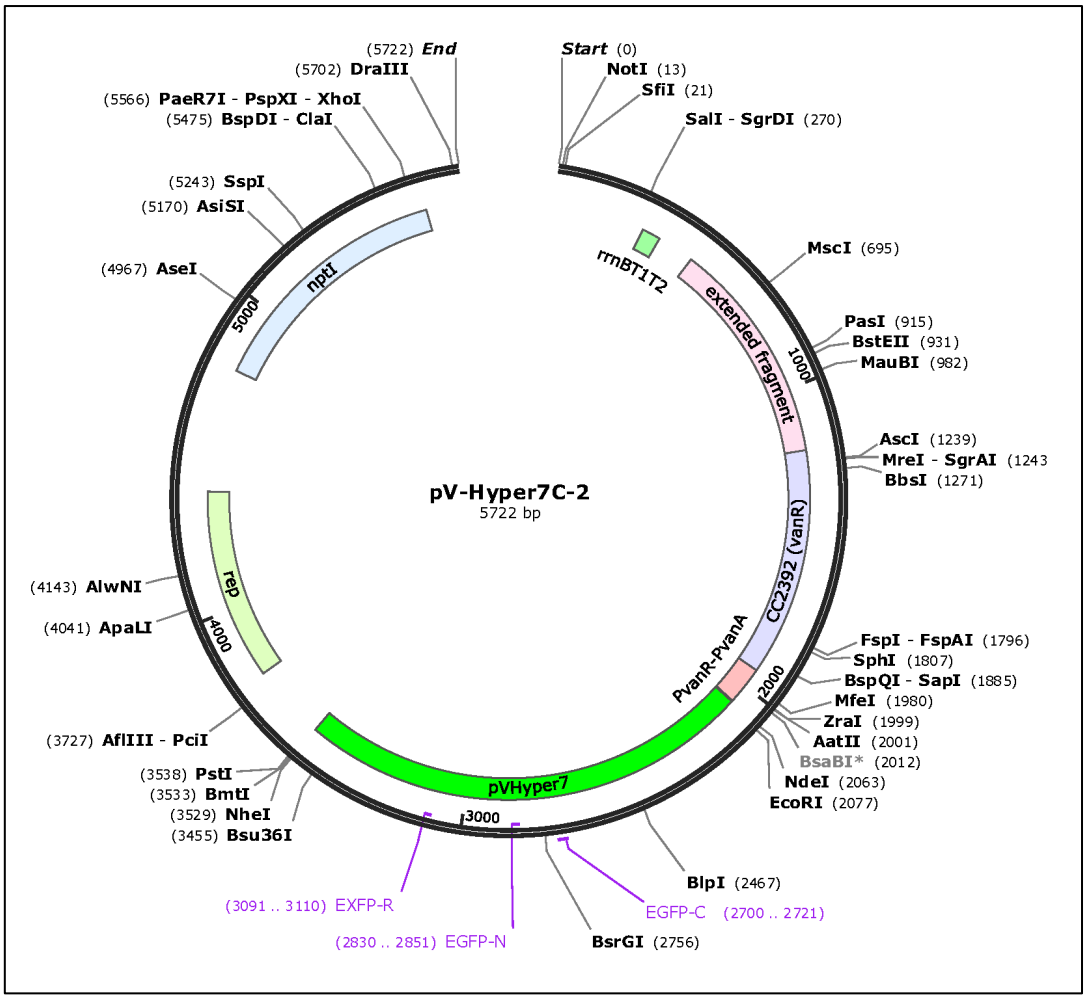

Figure 3. 20: Vector map of designed pVHyper7C-2 construct. The schematics shows the design of *C. crescentus* compatible integrative plasmid with Hyper7 between NdeI and NheI downstream to vannilate promoter (5722 bp) (drawn using SnapGene).

3.4.2 Preparation of pV-Hyper7C-2 construct and its integration into the *C. crescentus* genome

The Hyper7 gene composed of OxyR-RD fused with cpYFP in between OxyR-RD (1464 bp) is amplified from the template plasmid pQE30-HyPer7 (**Fig. 3.21 a**). The obtained amplicon (1464 bp) was digested, and ligated into the vector pVVENC2 and further transformed into EC100 cells (**Fig. 3.21 b**). The colonies obtained after transformation were screened for cells harbouring pV-Hyper7C-2 construct (**Fig. 3.21 c**).

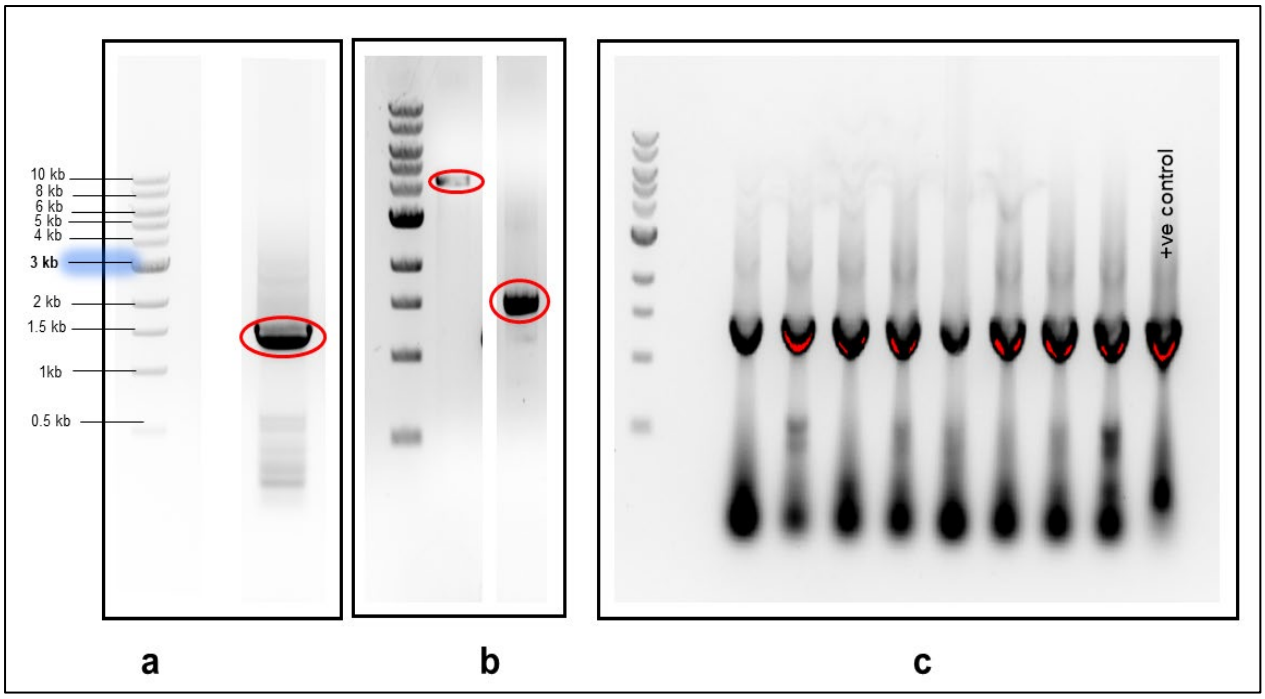

Figure 3. 21: Preparation of pV-Hyper7C-2 construct. The figure shows the agarose gel image for **a.** the PCR amplified product of the Hyper7 gene (1.46 kb). **b.** Restriction digested product of Hyper7 (left) and the plasmid pVVENC2 (4.258 kb) (right) with NdeI and NheI. **c.** the PCR screened EC100 colonies transformed with pVHyper7C-2. The requisite bands (1.46 kb) obtained were shown in all colonies representing EC100 containing pV-Hyper7C-2 construct. Last lane is positive control that represents the amplification of Hyper7 from the pQE30-HyPer7 with the requisite band 1.46 kb.

Currently, we are in process of integrating the confirmed pV-Hyper7C-2 into NA1000 genome. Once it is integrated further validation and measurement of H_2O_2 levels during the cell cycle in *C. crescentus* would be conducted.

Chapter 4 : **Discussion**

We have successfully constructed pV-Peredox_mCherryC-2, pVNADP-SnifitC-2, pVPercevalHRC-2 and pVHyper7C-2 to measure intracellular NAD(H), NADP(H), ATP-ADP ratio and H_2O_2 respectively. The efficiency of pV-Peredox-mCherryC-2 and pVPercevalHRC-2 has been validated in live *Caulobacter* cells. Furthermore, these genetically encoded sensors have been used to measure the NAD(H) and ATP/ADP levels during the cell cycle in synchronised population of *Caulobacter* cells. Interestingly, we observed that NADH/NAD^+ ratio remains constant till mid S-phase and significantly increases from mid-S phase onwards.

Furthermore, experiments using the pVPercevalHRC-2 construct indicated a decrease in ATP-ADP ratio upon entry into S-phase. This observation may suggest higher utilization of ATP in S-phase entry, which could be linked to activation of replication and proliferation. However, further experiments are required to validate this observation.

The genetically encoded sensors designed in this work can be used to monitor cell cycle abundance of nucleotides. Furthermore, these sensors can be used to study the influence of nutrients on cytoplasmic redox and its regulation during the cell cycle.

References

Benz, R, and McLaughlin, S (1983). The molecular mechanism of action of the proton ionophore FCCP (carbonylcyanide p-trifluoromethoxyphenylhydrazone). Biophysical Journal 41, 381–398.

Carmel-Harel, O, and Storz, G (2000). Roles of the Glutathione- and Thioredoxin-Dependent Reduction Systems in the *Escherichia Coli* and *Saccharomyces Cerevisiae* Responses to Oxidative Stress. Annu Rev Microbiol 54, 439–461.

Curtis, PD, and Brun, YV (2010). Getting in the Loop: Regulation of Development in *Caulobacter crescentus*. Microbiol Mol Biol Rev 74, 13–41.

Ely, B (1991). [17] Genetics of Caulobacter crescentus. In: Methods in Enzymology, Academic Press, 372–384.

Eun, Y-J, Foss, MH, Kiekebusch, D, Pauw, DA, Westler, WM, Thanbichler, M, and Weibel, DB (2012). DCAP: A Broad-Spectrum Antibiotic That Targets the Cytoplasmic Membrane of Bacteria. J Am Chem Soc 134, 11322–11325.

Green, J, and Paget, MS (2004). Bacterial redox sensors. Nat Rev Microbiol 2, 954–966.

Hu, Q, Wu, D, Walker, M, Wang, P, Tian, R, and Wang, W (2021). Genetically encoded biosensors for evaluating NAD+/NADH ratio in cytosolic and mitochondrial compartments. Cell Reports Methods 1, 100116.

Hung, YP, Albeck, JG, Tantama, M, and Yellen, G (2011). Imaging Cytosolic NADH-NAD+ Redox State with a Genetically Encoded Fluorescent Biosensor. Cell Metabolism 14, 545–554.

Imlay, JA (2002). How oxygen damages microbes: Oxygen tolerance and obligate anaerobiosis. In: Advances in Microbial Physiology, Elsevier, 111–153.

Lowry, OH, Passonneau, JV, Schulz, DW, and Rock, MK (1961). The Measurement of Pyridine Nucleotides by Enzymatic Cycling. Journal of Biological Chemistry 236, 2746–2755.

Messner, KR, and Imlay, JA (1999). The Identification of Primary Sites of Superoxide and Hydrogen Peroxide Formation in the Aerobic Respiratory Chain and Sulfite Reductase Complex of Escherichia coli. Journal of Biological Chemistry 274, 10119–10128.

Narayanan, S, Janakiraman, B, Kumar, L, and Radhakrishnan, SK (2015). A cell cycle-controlled redox switch regulates the topoisomerase IV activity. Genes Dev 29, 1175–1187.

Pak, VV, Ezeriņa, D, Lyublinskaya, OG, Pedre, B, Tyurin-Kuzmin, PA, Mishina, NM, Thauvin, M, Young, D, Wahni, K, Martínez Gache, SA, *et al.* (2020). Ultrasensitive Genetically Encoded Indicator for Hydrogen Peroxide Identifies Roles for the Oxidant in Cell Migration and Mitochondrial Function. Cell Metabolism 31, 642-653.e6.

Ray, PD, Huang, B-W, and Tsuji, Y (2012). Reactive oxygen species (ROS) homeostasis and redox regulation in cellular signaling. Cellular Signalling 24, 981–990.

Sallin, O, Reymond, L, Gondrand, C, Raith, F, Koch, B, and Johnsson, K (2018). Semisynthetic biosensors for mapping cellular concentrations of nicotinamide adenine dinucleotides. eLife 7, e32638.

Shapiro, L, Agabian-Keshishian, N, and Bendis, I (1971). Bacterial Differentiation. Science 173, 884–892.

Sporer, AJ, Kahl, LJ, Price-Whelan, A, and Dietrich, LEP (2017). Redox-Based Regulation of Bacterial Development and Behavior. Annu Rev Biochem 86, 777–797.

Tantama, M, Martínez-François, JR, Mongeon, R, and Yellen, G (2013). Imaging energy status in live cells with a fluorescent biosensor of the intracellular ATP-to-ADP ratio. Nat Commun 4, 2550.

Thanbichler, M, Iniesta, AA, and Shapiro, L (2007). A comprehensive set of plasmids for vanillate- and xylose-inducible gene expression in Caulobacter crescentus. Nucleic Acids Research 35, e137–e137.

Umemura, K, and Kimura, H (2005). Determination of oxidized and reduced nicotinamide adenine dinucleotide in cell monolayers using a single extraction procedure and a spectrophotometric assay. Analytical Biochemistry 338, 131–135.

Vidugiriene, J, Leippe, D, Sobol, M, Vidugiris, G, Zhou, W, Meisenheimer, P, Gautam, P, Wennerberg, K, and Cali, JJ (2014). Bioluminescent Cell-Based NAD(P)/NAD(P)H Assays for Rapid Dinucleotide Measurement and Inhibitor Screening. ASSAY and Drug Development Technologies 12, 514–526.

Wang, M, Da, Y, and Tian, Y (2023). Fluorescent proteins and genetically encoded biosensors. Chem Soc Rev 52, 1189–1214.

Xie, N, Zhang, L, Gao, W, Huang, C, Huber, PE, Zhou, X, Li, C, Shen, G, and Zou, B (2020). NAD+ metabolism: pathophysiologic mechanisms and therapeutic potential. Sig Transduct Target Ther 5, 227.

Yildiz, Ö, Kalthoff, C, Raunser, S, and Kühlbrandt, W (2007). Structure of GlnK1 with bound effectors indicates regulatory mechanism for ammonia uptake. EMBO J 26, 589–599.